

Identification of Positive Allosteric Modulators of Acetylcholinesterase for Treatment against
Organophosphorus Poisoning

Research Thesis

Presented in Partial Fulfillment of the Requirements for graduation

“with Research Distinction” in the undergraduate colleges of The Ohio State University

By

Kyle Burns

The Ohio State University

April 2021

Project Advisor: Dr. Craig McElroy, Division of Medicinal Chemistry and Pharmacognosy,
College of Pharmacy

Second Project Advisor: Dr. Christopher Hadad, Department of Chemistry and Biochemistry,
College of Arts and Sciences

Abstract

Acetylcholinesterase (AChE) is an enzyme that catalyzes the conversion of the neurotransmitter acetylcholine (ACh) into acetate and choline. ACh binds to muscarinic and nicotinic acetylcholine receptors triggering muscle contraction or neuronal communication.

Organophosphorus (OP) nerve agents and pesticides inhibit and/or age the active site of AChE.

AChE inhibition is the process by which the OP compound forms a covalent bond with the active site serine, whereas aging is the dealkylation of the OP moiety in the OP-AChE complex after inhibition. After inhibition and/or aging of AChE, a buildup of ACh in the synaptic clefts and neuromuscular junctions occurs, an event known as a cholinergic crisis, which causes severe harm and even death to an untreated individual. Currently approved therapeutics reactivate inhibited AChE, but they do not resurrect, or return to normal function, the aged form of the enzyme. Additionally, these positively charged therapeutics are incapable of crossing the blood-brain barrier, which is impermeable to charged molecules. Therefore, novel therapeutics must be developed to improve the treatment of OP poisoning. One approach to reducing the severity of OP poisoning is through the use of positive allosteric modulators of AChE. In general, a positive allosteric modulator (PAM) binds to an enzyme at a location removed from the active site and modifies the enzyme in a manner that increases its catalytic rate. Utilizing PAMs of AChE would enable remaining native AChE to increase the rate of conversion from ACh to acetate and choline, reducing the amount of AChE required to prevent cholinergic crisis. The modification of AChE caused by PAMs might also prevent OP agents from reacting with the active site serine or slow the rate of reaction. Further, the modifications caused by PAMs could potentially enhance the reactivation and/or resurrection of inhibited or aged AChE. Therefore, the initial goal of this project was to 1) identify novel PAMs of AChE, 2) test the identified compounds for prophylactic capabilities, and 3) identify which PAMs enhance the rate of reactivation and/or resurrection of AChE. However, a number of obstacles were encountered that question the results of previous work.

Acknowledgements

First, I would like to thank Dr. Craig McElroy for his guidance, not just during my thesis work, but before as well. Despite entering his lab with little experience, he patiently worked with me until I understood the project and the techniques that I would be utilizing. His knowledge of instrumentation is incredible and inspires me to reach outside my comfort zone so that I can hopefully be an expert in a variety of instrumentation methods one day. Dr. McElroy's mentorship has helped me gain confidence in my lab abilities and the confidence to pursue a career in research.

I would also like to thank Dr. Christopher Hadad for his support over the course of my undergraduate research career. His advice on my work, including this project, and his willingness to serve as a second project advisor and committee member is greatly appreciated. Finally, I would like to thank the members of the McElroy and Hadad labs, especially Garima Agarwal, Steven Ratigan, and Gopichand Gutti. Garima, Steven, and Gopichand have helped me out numerous times in the lab and answered many of my questions during my time in the McElroy lab.

Table of Contents

Background.....	1
Role of Acetylcholine in the Body.....	1
Structure of Acetylcholinesterase.....	2
Organophosphorus Nerve Agents and Pesticides.....	3
Organophosphorus Poisoning and Treatment.....	6
Materials and Methods.....	11
Enzyme.....	11
Compound Library.....	11
Synthesis of A3.....	15
Solvation of Test Compounds.....	15
Dose-Response Assays.....	17
Solvent Dose-Response.....	17
Compound Dose-Response.....	18
Single-Point Test.....	22
Data Analysis.....	22
Results.....	23
Solvent Dose-Response.....	23
Compound Dose-Response.....	24
Single-Point Test.....	36
Discussion.....	39
References.....	47

Figure 1: Synthesis of Acetylcholine (Meriney & Fanselow, 2019)	1
Figure 2: Structures of Acetylcholine receptor agonists	2
Figure 3: AChE hydrolysis of ACh (Franjesevic et al., 2019).....	2
Figure 4: Silhouette of AChE shown in white with gorge labeled (Franjesevic et al., 2019).....	3
Figure 5: Structures of OP Nerve Agents	4
Figure 6: Structures of OP Pesticides.....	5
Figure 7: Mnemonic device for symptoms of OP poisoning (Gupta, 2015).....	6
Figure 8: Mechanism of OP Inhibition and Aging (Franjesevic et al., 2019).....	6
Figure 9: Compounds based on Chapleau et al. pharmacophores (red)	13
Figure 10: Compounds from the Chapleau et al. (2015) experiments	14
Figure 11: FDA-approved drugs that showed activation in Katz et al. (2018)	14
Figure 12: Precipitation and plate map from the solvent dose-response assay	27
Figure 13: Results from the third assay	28
Figure 14: Results from the fourth assay	29
Figure 15: Results from the fifth assay (1-hour incubation).....	29
Figure 16: Results from the fifth assay (2-hour incubation).....	30
Figure 17: Results from the sixth assay	31
Figure 18: Results from the seventh assay (Part 1).....	31
Figure 19: Results from the seventh assay (Part 2).....	32
Figure 20: Results from the seventh assay (part 3).....	32
Figure 21: Results from the eighth assay (part 2)	34
Figure 22: Results from the eighth assay (part 3)	34
Figure 23: Results from the eighth assay (part 4)	35
Figure 24: Results from the ninth assay (part 1).....	35
Figure 25: Results from the ninth assay (part 3).....	36
Figure 26: Results from the ninth assay (part 2).....	36
Figure 27: Results from the tenth assay (part 1)	37
Figure 28: Results from the ninth assay (part 4).....	37
Figure 29: Results from the tenth assay (part 2)	38
Figure 30: Results from the 11th assay (part 1).....	39
Figure 31: Results from the 11th assay (part 2).....	39
Figure 32: Results from the 125-uM single-point assay	40
Figure 33: Results from the 250-uM single-point assay	41
Figure 34: Precipitation and plate map from single-point assays	42
 Scheme 1: Synthesis of A3 from para-aminophenol	 15
 Table 1: Lists of Solvents used in Dissolving Test Compounds	 16
Table 2: Summary of the Compound Dose-Response Assays Performed	25

Background

Role of Acetylcholine in the Body

Acetylcholine, the first neurotransmitter to be discovered (Meriney & Fanselow, 2019), is found in the autonomic, somatic, and central nervous systems where it is synthesized by presynaptic neurons (**Figure 1**).

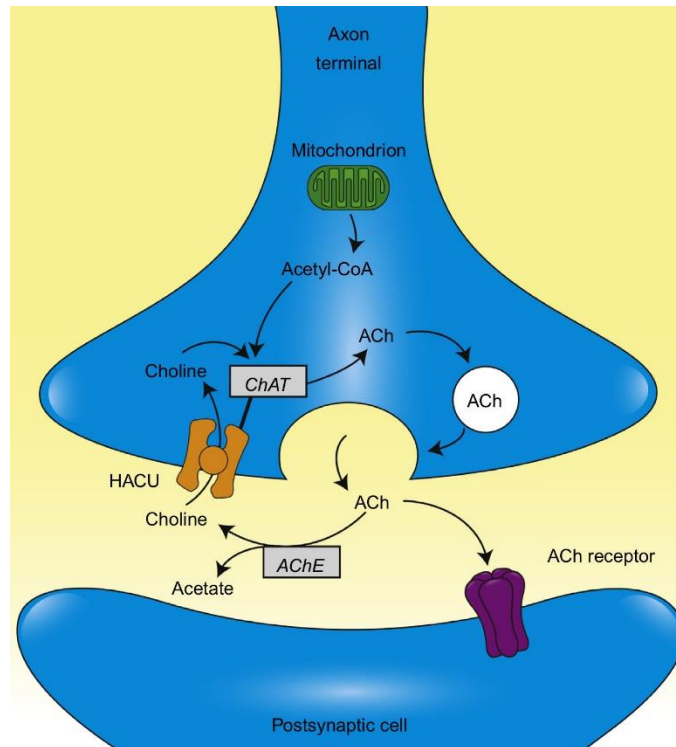


Figure 1: Synthesis of Acetylcholine - Choline acetyltransferase (ChAT) combines choline and acetyl-CoA to form acetylcholine. Acetylcholine (ACh) is then stored in vesicles that merge with the synaptic membrane to release ACh into the synapse. Acetylcholinesterase (AChE) hydrolyzes ACh into acetate and choline. High-affinity, low-efficiency choline uptake transporters (HACU) transport the resulting choline back into the presynaptic neuron. (Meriney & Fanselow, 2019)

In the central nervous system, acetylcholine is synthesized in the basal forebrain nuclei and the mesopontine tegmental area of the brain. Although the role of acetylcholine in the brain is not fully understood, it is thought to play a role in arousal, attention, and memory. However, in the rest of the body, acetylcholine serves to induce muscle contraction in the neuromuscular junctions by triggering the uptake of sodium into the muscle cell and releasing potassium. Two acetylcholine receptors are important in the neurotransmitter activity: muscarinic and nicotinic

receptors. The names of these receptors originate from the chemicals they bind in addition to acetylcholine. Muscarinic receptors bind muscarine, and nicotinic receptors bind nicotine (**Figure 2**).

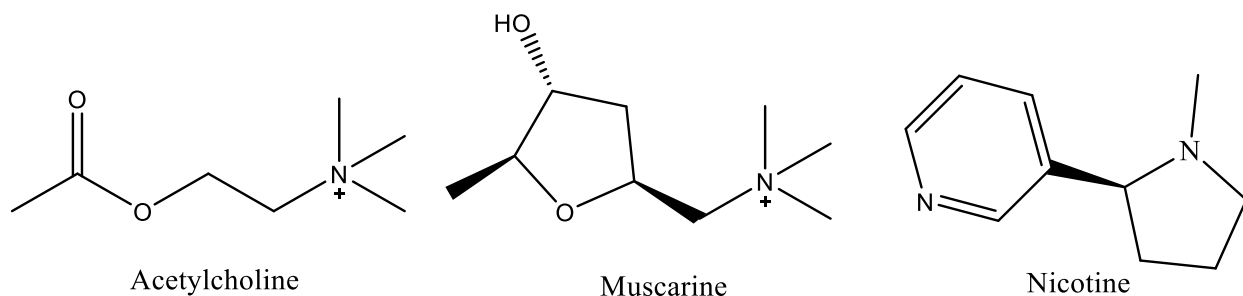


Figure 2: Structures of Acetylcholine receptor agonists

To control the activation of acetylcholine receptors, the acetylcholinesterase (AChE) enzyme catalyzes the conversion of ACh into acetate and choline (**Figure 1; Figure 3**).

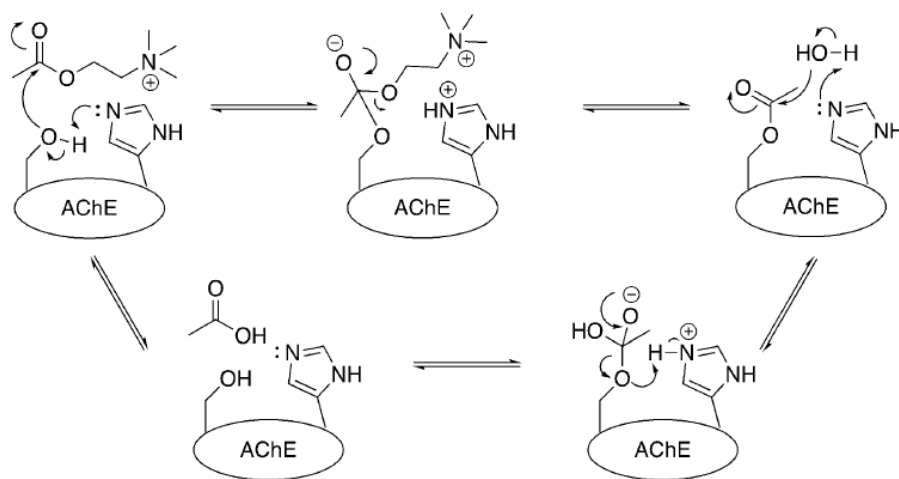


Figure 3: AChE hydrolysis of ACh (Frajesevic et al., 2019)

Structure of Acetylcholinesterase

AChE exists in many isoforms depending on the species (human, mouse, eel, etc.) and where it is located in the body (synaptic cleft, neuromuscular junction, erythrocyte, etc.). Globular AChE can exist as a monomer, dimer, or tetramer (Sakayanathan et al., 2019). One common characteristic of an AChE subunit is the narrow gorge that is 0.75 to 2.5 angstroms

wide and 20 angstroms deep (Franjesevic et al., 2019; **Figure 4**). The mouth of the gorge is home to the peripheral anionic site (PAS) that interacts with the choline segment of ACh to thrust the substrate into the catalytic site.

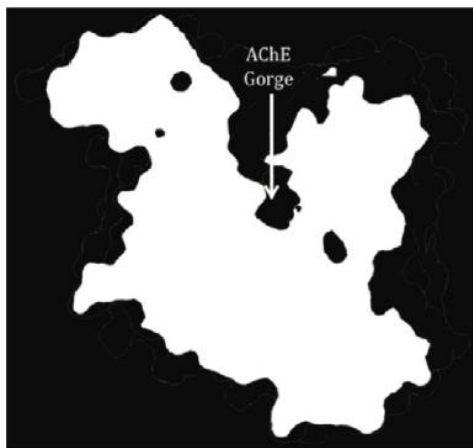


Figure 4: Silhouette of AChE shown in white with gorge labeled (Franjesevic et al., 2019)

Inhibition of AChE has been shown to be a therapeutic approach for treating symptoms of certain illnesses such as Alzheimer's Disease (AD) and myasthenia gravis. Donepezil, rivastigmine, and galantamine treat AD, whereas pyridostigmine bromide treats myasthenia gravis. Unfortunately, AChE is also the target of many organophosphorus nerve agents and pesticides.

Organophosphorus Nerve Agents and Pesticides

Since Gerhard Schrader stumbled upon tabun while developing insecticides in 1936, many nations have pursued organophosphorus nerve agents as part of their chemical weapons programs (Franjesevic et al., 2019). Germany developed tabun (GA), sarin (GB), soman (GD), and cyclosarin (GF); the United States developed VX; and Russia developed VR and several Novichok agents (**Figure 5**).

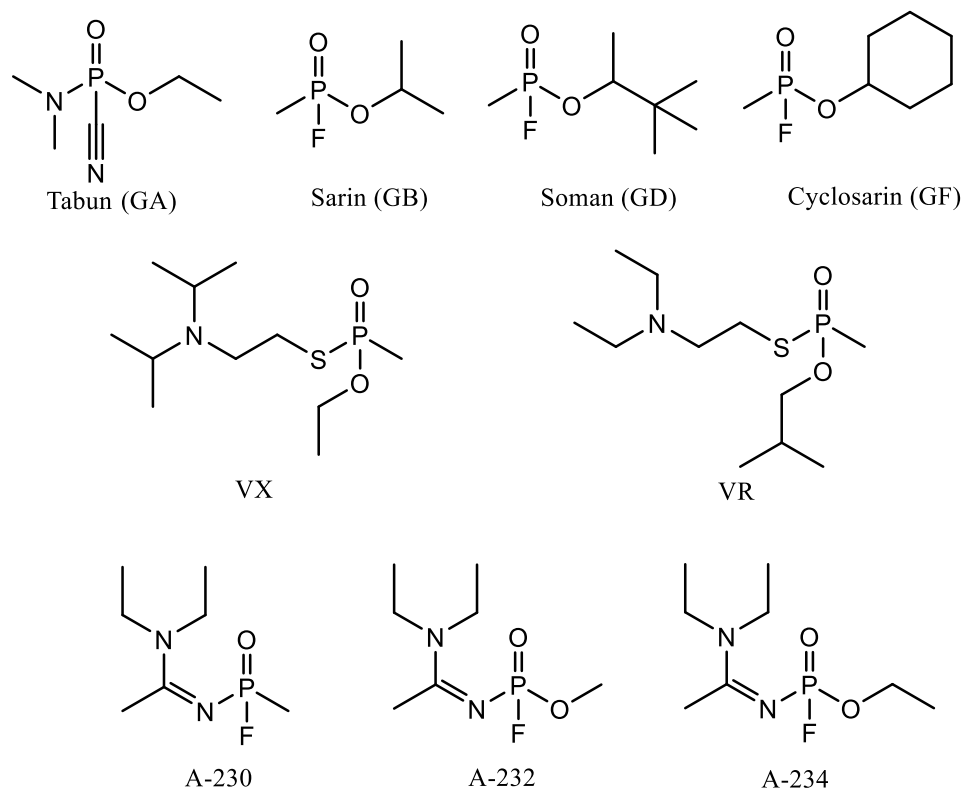


Figure 5: Structures of OP Nerve Agents - G-series (Top), V-series (Middle), and Novichok Agents (Bottom)

Of course, these chemicals have not remained isolated in the countries where they were developed. For example, in the 1980s, Iraq used hundreds of tons of sarin and tabun against Iranian troops affecting over 100,000 people (Franjesevic et al., 2019). In 2013 and 2017, the Syrian government used sarin on rebel forces, killing and injuring close to 2,000 people between the two incidents (Franjesevic et al., 2019). Even more recently, Russia has been under scrutiny by the United Nations for utilizing Novichok agents to carry out assassinations, or assassination attempts, like that on President Vladimir Putin’s political rival Alexei Navalny (“Russia responsible,” 2021).

Outside of the militarization of nerve agents, they have also become a powerful tool for terrorist organizations. The danger of these agents in the hands of terrorists can be seen in the Matsumoto attack of 1994 and the Tokyo subway attack of 1995 (Gupta, 2020). On June 27,

1994, sarin gas was dispersed in Matsumoto City, Japan killing eight people and hospitalizing many others. Following this attack, in 1995, a cult released homemade liquid sarin on a subway killing 13 people and hospitalizing over 5000. However, had the sarin been in the gas phase like the Matsumoto attack, it is likely the death toll would have been much higher (Franjesevic et al., 2019).

In agriculture, organophosphorus pesticides have been popular for protecting crops despite the known risks associated with their use. As of 2012, approximately one third of all insecticides used annually in the United States were organophosphorus compounds (Atwood & Paisley-Jones, 2017). Examples of these pesticides include acephate, chlorpyrifos, diazinon, malathion, and parathion (**Figure 6**).

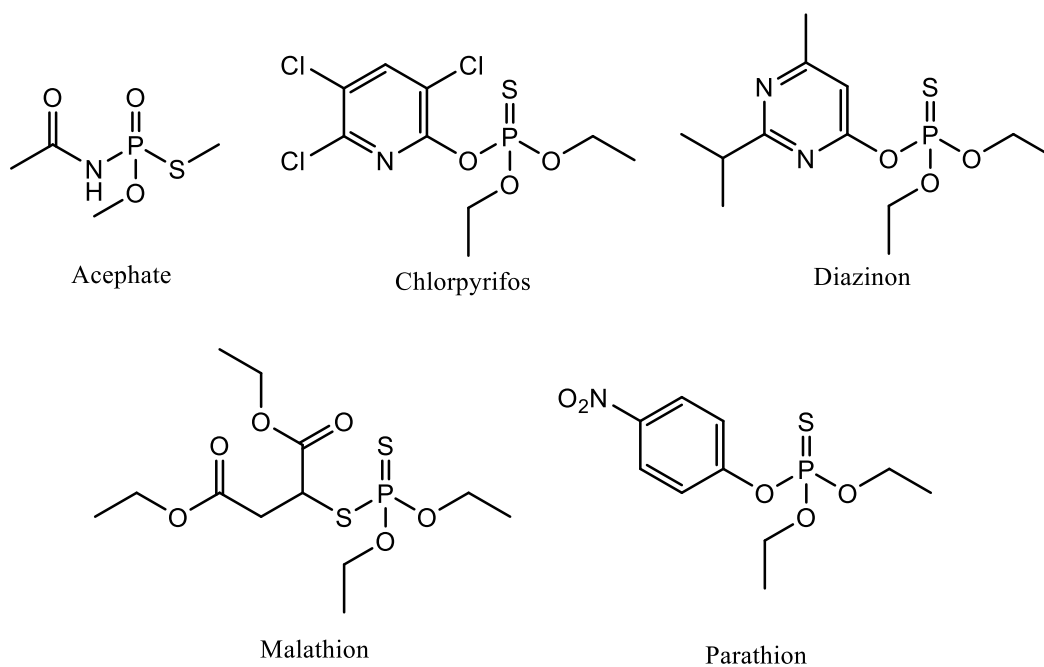


Figure 6: Structures of OP Pesticides

Organophosphorus Poisoning and Treatment

Poisoning by organophosphorus nerve agents or pesticides results in a variety of severe symptoms, some of which comprise the mnemonic SLUDGE: salivation, lacrimation, urination, defecation, gastric cramps, and emesis (Peter et al., 2014). However, a more comprehensive mnemonic device for the symptom of OP poisoning is BAG the PUDDLES (**Figure 7**).

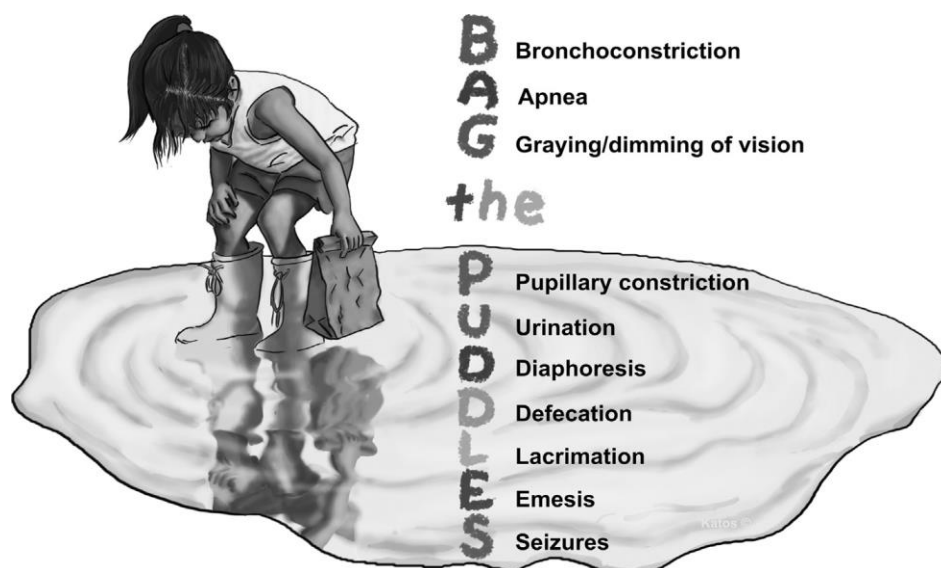


Figure 7: Mnemonic device for symptoms of OP poisoning (Gupta, 2015)

The mechanism by which organophosphorus nerve agents and pesticides elicit these symptoms is through their reaction with AChE and involves two steps. The first step involves the formation of a covalent bond with the active site serine forming inhibited AChE (**Figure 8**). The

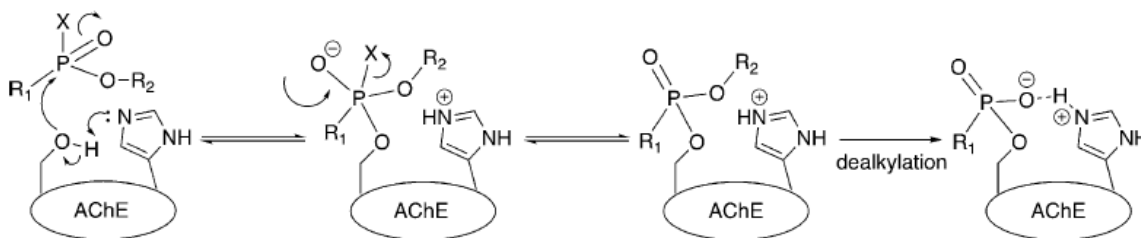


Figure 8: Mechanism of OP Inhibition and Aging (Franjesevic et al., 2019)

second is an enzyme-catalyzed dealkylation of the organophosphorus moiety of the OP-AChE complex which is known as aging.

In both inhibited and aged AChE, the enzyme can no longer convert ACh to acetate and choline. This results in a buildup of the neurotransmitter in the synaptic cleft or neuromuscular junction leading to a cholinergic crisis where the excess of ACh leads to an increased rate of binding and activation of the acetylcholine receptors.

To treat the resulting symptoms, atropine, diazepam, and an AChE reactivator are given to the poisoned patient. Atropine acts as a competitive antagonist of muscarinic ACh receptors, reducing the activation of these receptors by the excess of ACh (Rotenberg & Newmark, 2003). Diazepam is a benzodiazepine that serves to allosterically enhance binding of the inhibitory neurotransmitter GABA to GABA_A receptors, thereby reducing or preventing seizures resulting from the cholinergic crisis. Since neither atropine nor diazepam restore the native function of AChE, reactivators such as 2-PAM, which is approved for use in the United States, HI-6, or obidoxime are administered to restore the native function of AChE from the OP-inhibited state. Unfortunately, there are no currently approved therapeutics that resurrect aged AChE or sufficiently cross the blood-brain barrier to restore brain AChE function. Although resurrecting AChE has proven to be more difficult, there have been leads in developing resurrectors that accomplish this task (Franjesevic et al., 2019).

Introduction

The currently approved treatment options for OP poisoning are primarily post-exposure therapeutics. The clear downsides to these approaches are that the patient still endures severe symptoms prior to treatment with a reactivator and/or endures long-lasting effects from the OP agents if there is significant absorption of the OP into the brain (Gupta, 2020). An alternative approach would be through a prophylactic, pre-exposure treatment that would prevent or limit the severe symptoms a patient would experience. While they are more likely to be effective post-exposure, one such approach could be through the use of positive allosteric modulators of AChE. In general, a positive allosteric modulator (PAM) binds to an enzyme away from the active site and modifies the enzyme in a manner that increases its catalytic rate. The catalytic rate (k_{cat}) of native AChE is approximately 25,000 molecules of ACh per second with a catalytic efficiency (k_{cat}/K_M) of $1.50 \times 10^9 \text{ M}^{-1} \text{ s}^{-1}$ (Colovic et al., 2013). With such a high efficiency, it is reasonable for the PAM approach to be met with skepticism. However, there have been a number of studies suggesting that the rate of ACh hydrolysis can be increased while maintaining the K_M , thereby increasing the efficiency of the enzyme (Reiner & Simeon-Rudolf, 2000; Grifman et al., 1997; Alvarez et al., 1998). Further, a number of allosteric binding sites have been identified through computational approaches (Roca et al., 2018). This potential for PAMs to bind to AChE and increase the rate of hydrolysis of ACh provides an obvious avenue for treatment. If PAMs are administered post-exposure, the remaining native AChE would have an increase in the rate of conversion of ACh, reducing the amount of AChE required to prevent the cholinergic crisis. If the effective activity of AChE is increased above 20%, then the patient would no longer experience severe symptoms (Colovic et al., 2013). As the percent of effective AChE activity increases, the patient's symptoms in theory would reduce even more. This approach has the

potential to be extremely effective when combined with the current standard of care for OP poisoning, especially considering the reactivation abilities of 2-PAM and HI-6 (Franjesevic et al., 2019). Provided the PAMs can cross the blood-brain barrier, then the effective activity of brain AChE could also be increased, protecting the central nervous system. However, if PAMs modify AChE causing an increase in the rate of hydrolysis of ACh, they may also affect the inhibition rate by OPs, potentially reducing the rate of inhibition. Reducing the inhibition rate of AChE by OPs could provide a pre-exposure prophylactic for soldiers who may come in contact with an OP nerve agent or agriculture workers who may come into contact with higher concentrations of OP pesticides, protecting individuals against severe symptoms and even death after exposure. Prochlorperazine, an FDA-approved antipsychotic, was demonstrated to have this capability *in vitro* but there are no PAMs that have been shown to have this effect in humans yet (Katz et al., 2018). Additionally, even if given post-exposure, if the rate of inhibition by OPs is reduced, PAMs would protect the remaining uninhibited enzyme from becoming inhibited. Another potential benefit of this treatment approach is that the modification of AChE caused by PAMs might prevent OP metabolites, whether from normal processes or reactivation of AChE, from interacting with the active site serine. Further, the modifications could also enhance the reactivation and/or resurrection of inhibited or aged AChE either through rate enhancement or increasing the uptake of the therapeutic compound to the active site. Therefore, the purpose of this project was to utilize a modified Ellman's method *in vitro* to 1) identify novel PAMs of AChE through a dose-response assay, 2) test the identified compounds for prophylactic capabilities via a protection assay, and 3) identify which PAMs enhance the rate of reactivation and/or resurrection of AChE by their respective assays. Unfortunately, a number of issues were

encountered that stalled the progress of this study and herein only the dose-response assay is discussed.

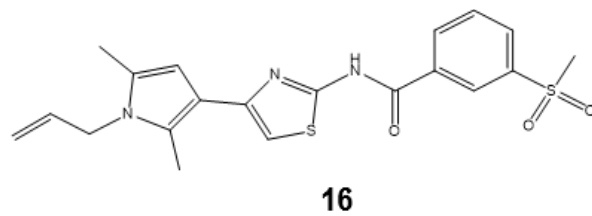
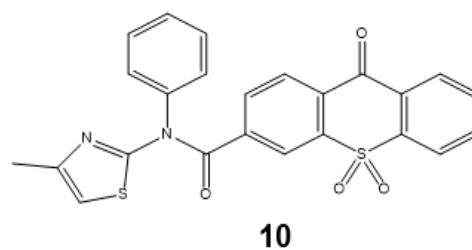
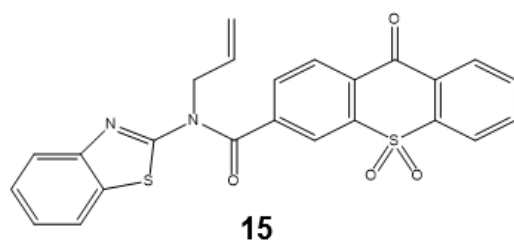
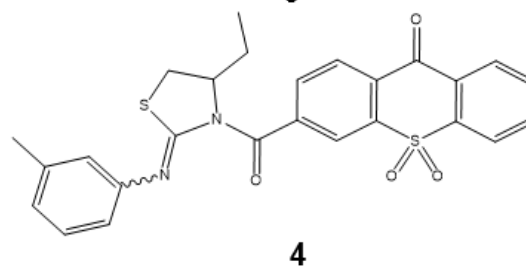
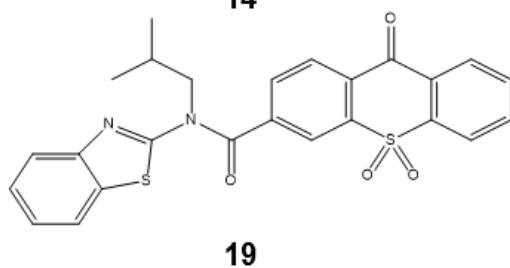
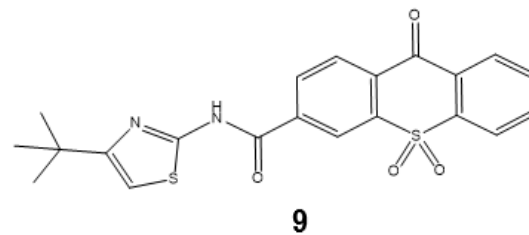
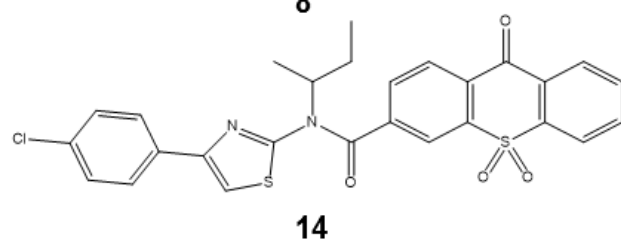
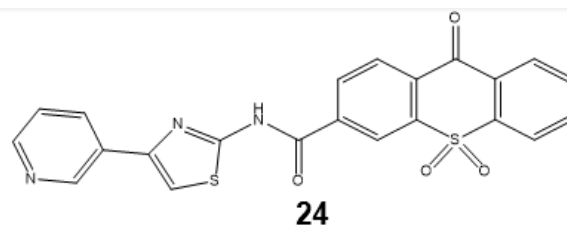
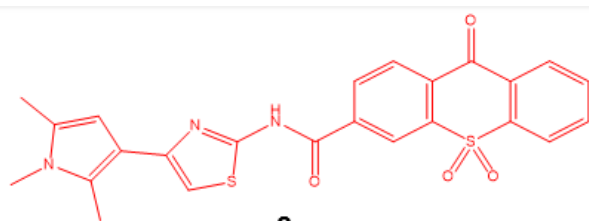
Materials and Methods

Enzyme

The AChE used in these experiments was generously provided by Dr. Zoran Radic from the University of California San Diego. It is a recombinant human isoform of the enzyme consisting of only the catalytic core expressed in HEK293 cells.

Compound Library

A library consisting of several sets of compounds were purchased to develop a structure-activity relationship (SAR). The first set was purchased from Enamine and consisted of 27 compounds (**Figure 9**). This set was planned around compounds (in red) that had previously been shown to activate AChE. Specifically, these compounds were identified by the high-throughput screening during the Chapleau et al. (2015) experiments and demonstrated a dose-response PAM activity. The purchased compounds have varying substituents on the potential pharmacophores.



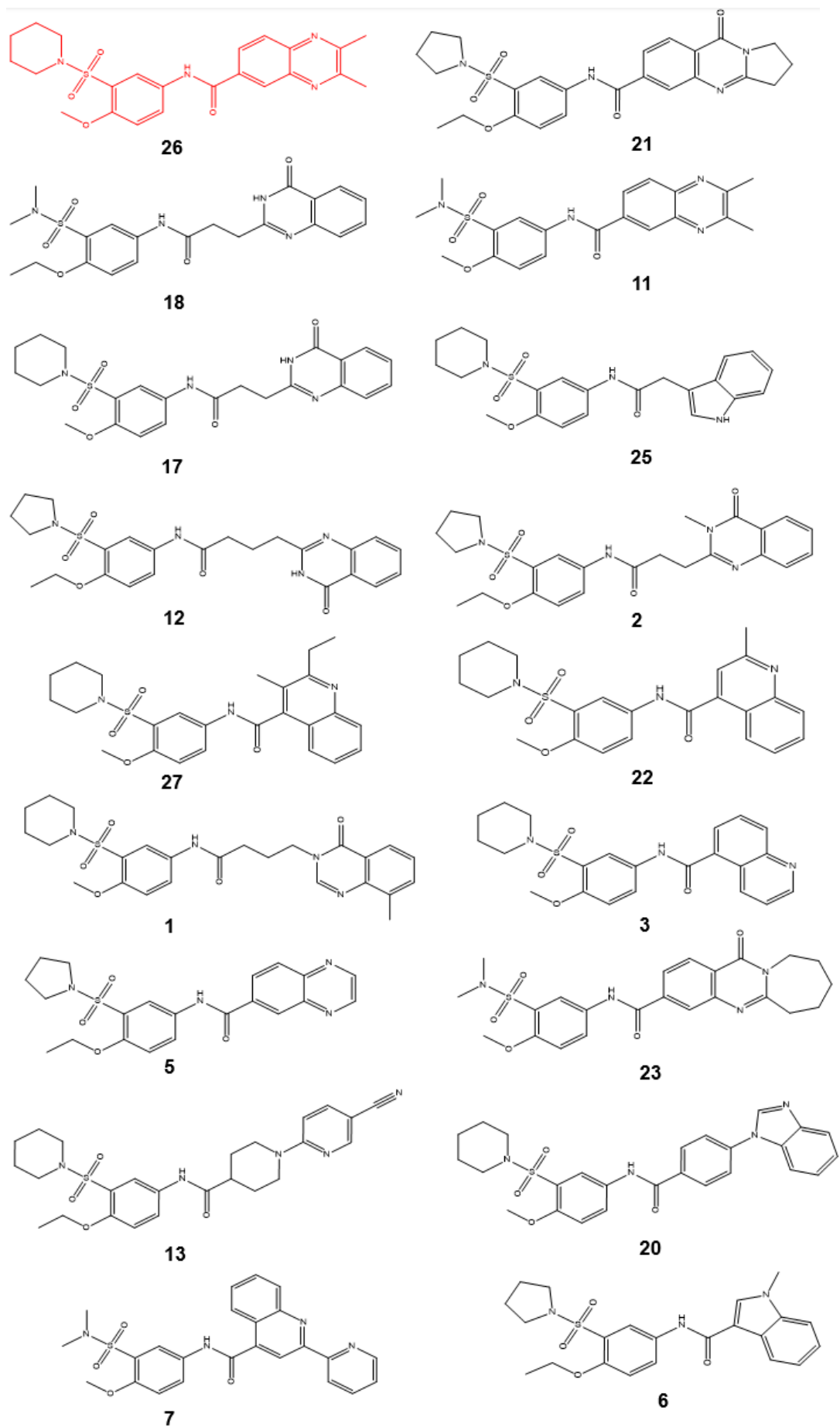


Figure 9: Compounds based on Chapleau et al. pharmacophores (red)

The second set was provided by Dr. Craig McElroy and consisted of compounds also from the Chapleau et al. (2015) experiments (**Figure 10**).

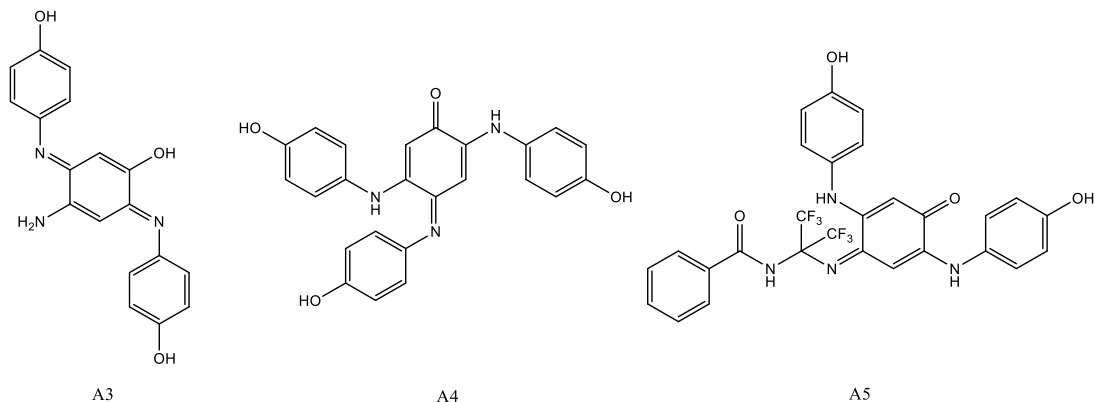


Figure 10: Compounds from the Chapleau et al. (2015) experiments

Prior to this **A3** was resynthesized following a similar method which is detailed below. The A compounds were verified by NMR to have a purity above 95%, thanks to Garima Agarwal prior to use (data not shown). The last set was purchased based on the results of Katz et al. (2018; **Figure 11**). These compounds are all currently FDA-approved drugs and could provide an interesting lead in the development of another treatment against OP poisoning.

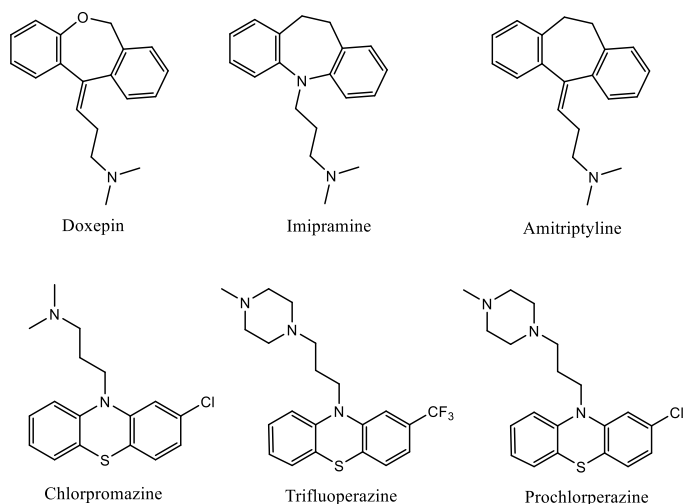
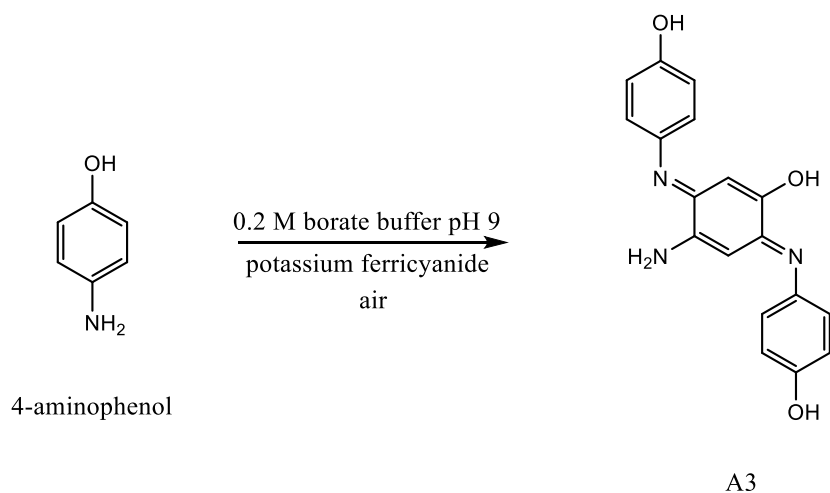


Figure 11: FDA-approved drugs that showed activation in Katz et al. (2018)

Synthesis of A3

After preparing 100 mM borate buffer at pH 9, 1.98 grams of *p*-aminophenol was dissolved while stirring for 20-30 minutes at room temperature. 2.01 grams of potassium ferricyanide was added and the reaction mixture turned black in color. Air was then bubbled through the reaction mixture at room temperature while being stirred until it was dry. The resulting black solid was filtered and washed with water before triturating into methanol. After evaporating the methanol, purified black **A3** remained (1.28 g, 66%).



Scheme 1: Synthesis of **A3** from para-aminophenol

Solvation of Test Compounds

Solvation of the test compounds for testing proved difficult and a large number of solvents were used in trying to dissolve compounds **1-27** to a concentration of 100 mM so that the final concentration of solvent in the assay was as low as possible. These solvents are listed below (**Table 1**).

An attempt was made to avoid or reduce the amount of dimethylsulfoxide (DMSO) used for solvation as it causes a decrease in AChE activity. Therefore, in addition to the individual solvents, a few binary solvent mixtures were also prepared by combining DMSO and acetone which does not demonstrate as much inhibition (Kumar & Darreh-Shori, 2017). Each attempt at dissolving the compounds consisted of vortexing the vials at 2500 rpm for an hour on a Benchmark BV1010 Multi-tube Vortexer. Although the vials were not placed in an incubator, the friction generated on the vortexer surprisingly led to a significant amount of heat. If the compounds did not dissolve, the solvent was evaporated on an Organomation MULTIVAP100 Nitrogen Evaporator or in a Genevac EZ-2 PLUS. If DMSO was a component of the solvent, the remaining DMSO was lyophilized using a Labconco Freezone 6 Lyophilizer. Unfortunately, only compounds **5**, **6**, **10**, **17**, and **23** dissolved at 100 mM in the binary solvent mixture solutions. The remaining compounds were not soluble enough to form 100 mM solutions in any of the solvents listed with some compounds appearing to be completely insoluble in all of the solvents. In fact, most were only soluble at 10 mM in DMSO. Eventually, to maintain uniformity, all compounds tested were dissolved at 10 mM in DMSO, including **5**, **6**, **10**, **17**, and **23** as well as the **A** compounds from the second set and the FDA-approved drugs from the third set.

Solvents
Acetone
Acetone:DMSO
Acetonitrile
Distilled Water
Distilled Water with 1% Formic Acid
DMSO
Ethanol
Isopropanol
Methanol

Table 1: Lists of Solvents used in Dissolving Test Compounds

Dose-Response Assays

A variety of dose-response assays were performed while attempting to determine the activation potencies of the test compounds. Each assay was modified slightly from the previous one in order to address the obstacles that are discussed below. In all of these assays, the final concentrations of acetylthiocholine (ATC) and 5,5'-dithiobis(2-nitrobenzoic acid) (DTNB) were 0.5 mM and 1 mM, respectively. If bovine serum albumin (BSA) was added, its final concentration was 0.09 g/L. ATC was prepared in water, DTNB was prepared in 20 mM Na_3PO_4 , and BSA was prepared in 200 mM sodium phosphate buffer at pH 7.5. Each assay also utilized 200 mM sodium phosphate buffer at pH 7.5 unless otherwise noted. The addition of ATC and DTNB was performed using the dispensing module on a Biotek Synergy H1 Hybrid plate reader followed by a 20-second linear shake prior to a sweep read at 412 nm. All other assay components were added using an Integra Assist Plus robotic liquid handler equipped with Integra Voyager pipettes and Low Retention pipette tips. AChE, BSA, ATC, and DTNB solutions were mixed on a Thermolyne RotoMix Single Speed Orbital Mixer for approximately 30 minutes before being used. AChE and BSA solutions were kept on ice during this time. ATC and DTNB solutions were vortexed for several minutes before being placed on the mixer.

Solvent Dose-Response

While attempting to dissolve the test compounds, the solvents with an unknown effect on AChE or the other assay materials were tested to determine their compatibility with the assay. Benzylamine, cyclohexanone, pyridine, and triethylamine were added so that their final concentrations (% v/v) were 10, 5, 2.5, and 1%. Phosphate buffer, distilled water, acetonitrile, and DMSO were included as controls. Each well contained AChE and BSA in phosphate buffer

before the test solvents were added. ATC and DTNB were then added using the dispensing module on the plate reader.

Compound Dose-Response

As noted above, a variety of dose-response assays were performed. Brief descriptions of each assay will be detailed here with a summary table at the end of this section (**Table 2**).

The first assay was performed by serially diluting the 100 mM stock solutions of compounds **5**, **6**, **10**, **17**, and **23** into 200 mM sodium phosphate buffer on a PCR plate with 2 mM as the highest concentration in the dilution series. Despite sufficient mixing, a precipitate formed in the initial wells upon the addition of the test compound solutions, including the 3:1 acetone-DMSO negative control.

The second assay utilized a direct, variable volume dilution method where three different volumes of 100 mM compound were dispensed into separate wells of 200 mM sodium phosphate buffer to achieve final concentrations of 1.00, 0.50 and 0.25 mM. These wells were then serially diluted five-fold into 200 mM sodium phosphate buffer. A negative control with a 3:1 acetone-DMSO solution was prepared in parallel. This assay also could not be completed due to the formation of precipitates in the dilution plate.

The third assay consisted of adding the AChE and BSA components to the 200 mM sodium phosphate buffer prior to three direct, variable volume dilutions of compounds **5**, **6**, **10**, **17**, **19**, **20**, and **23** at 10 mM in DMSO resulting in wells with final concentrations of 0.25, 0.10, and 0.05 mM. Each variable volume dilution was followed by a 10-fold serial dilution. The final relative activity of AChE was 0.0017 $\mu\text{mol}/\text{min}$ in each well. After incubating the plate at 37°C

for 30 minutes, ATC and DTNB were added and a sweeping, 10-minute kinetic read was performed at 412 nm.

Because the results of the third assay did not match those in the literature, the fourth assay took note of the method of Chapleau et al. (2015) where the test compounds were added by an Echo 550 liquid handler. To mimic this, small droplets of 10 mM compound in DMSO were added to empty wells before a pre-mixed solution of AChE and BSA in 200 mM sodium phosphate buffer was slowly added so that the relative activity of AChE was the same in each well. The wells were vigorously mixed before a five-fold dilution was performed. After incubating the plate at 37°C for 30 minutes, ATC and DTNB were added and a sweeping, 10-minute kinetic read was performed at 412 nm.

The fifth assay was a modification of the fourth assay. The incubation time was increased to 1 hour, and the concentration of AChE was reduced so that the relative activity in each well was 0.0004 $\mu\text{mol}/\text{min}$. Additionally, the number of direct, variable volume dilutions was decreased to two yielding concentrations of 50 μM and 25 μM . These wells were then serially diluted five-fold. Lastly, the contents of the 96-well plate were transferred to a 384-well format after incubation. The 384-well plate was then placed on the plate reader, and the 96-well plate was returned to the incubator while the 384-well plate was read. After another hour had passed, the 96-well plate was then read.

The sixth assay was a repeat of the fifth assay. However, instead of 200 mM phosphate buffer, 40 mM phosphate buffer was used. Additionally, only the one-hour incubation was performed.

The seventh assay was also similar to the fifth assay. Again, only the one-hour incubation was performed, and the final concentration was slightly greater yielding an activity of 0.0006 $\mu\text{mol}/\text{min}$ in each well.

After noticing the lower concentrations were still resulting in AChE activity similar to the negative DMSO control, the plate layout from the fifth through seventh assays was modified for the eighth assay to double the number of compounds tested per run using only the five greatest concentrations from the previous assays, starting with 50 μM . The AChE concentration was also lowered to yield a final activity of 0.0003 $\mu\text{mol}/\text{min}$ in each well.

Due to shipping delays, the 300 μL tips for the Integra Voyager were depleted during the course of the experiments so the 1250 μL pipette was used to dispense the appropriate volumes for the ninth through eleventh assays. The ninth assay was similar to the eighth assay, but the concentration of AChE was increased to yield an activity of 0.0021 $\mu\text{mol}/\text{min}$ in each well.

After acknowledging BSA was not included in either the Chapleau et al. (2015) or Katz et al. (2018) experiments, the tenth assay was a repeat of the ninth assay but excluded BSA to investigate the effect of BSA on the test compounds.

For the eleventh assay, AChE was incubated overnight (~13 hours) at 37°C in 200 mM sodium citrate buffer pH 6.0 to denature some of the enzyme. The activity of the incubated AChE was then tested with a non-incubated sample for comparison. The tenth assay procedure, which excluded the addition of BSA, was repeated afterwards.

Summary of Assays	1st Assay	2nd Assay	3rd Assay	4th Assay	5th Assay	6th Assay	7th Assay	8th Assay	9th Assay	10th Assay	11th Assay
Compound Droplet Added First?	No	No	No	Yes	Yes	Yes	Yes	Yes	Yes	Yes	Yes
Sodium Phosphate Buffer Conc. (mM)	200	200	200	200	200	40	200	200	200	200	200
Highest Conc. of Compound (uM)	2000	1000	250	50	50	50	50	50	50	50	50
Direct, Variable Volume Dilution then Serial Dilution?	No	Yes	Yes	Yes	Yes	Yes	Yes	Yes	Yes	Yes	Yes
Number of Direct Dilutions	-	3	3	2	2	2	2	2	2	2	2
Negative Control	3:1 acetone-DMSO	3:1 acetone-DMSO	DMSO	DMSO	DMSO	DMSO	DMSO	DMSO	DMSO	DMSO	DMSO
Pipette Used for Serial Dilution	300	300	300	300	300	300	300	300	1250	1250	1250
Incubation Time (hr)	-	-	0.5	0.5	18.2	1	1	1	1	1	1
Was BSA added?	Yes	Yes	Yes	Yes	Yes	Yes	Yes	Yes	Yes	No	No
Activity of Positive Control (umol/min)	-	-	0.0017	0.0017	0.0004	0.0004	0.0006	0.0003	0.0021	0.0021	0.0003
CV of Positive Control	-	-	4%	2%	5% & 4%	2%	3-7%	2% & 5%	30% & 29%	20%	34%

Table 2: Summary of the Compound Dose-Response Assays Performed

Single-Point Test

In addition to performing multiple dilution series, two single-point high concentration assays were also performed using the modified Ellman's method. The first was at a final compound concentration of 250 μ M in each well, resulting in a final DMSO concentration of 2.5% in phosphate buffer with AChE, before the addition of ATC and DTNB. No BSA was added to follow the methods of Chapleau et al. (2015) and Katz et al. (2018). To account for the inhibitory effect of DMSO on AChE, the inhibition curve of DMSO was used to calculate the amount of AChE needed to have a final relative activity of 0.002 units. The second assay was performed similarly with a final compound concentration of 125 μ M in each well resulting in a final DMSO concentration of 1.25% in phosphate buffer with AChE, before the addition of ATC and DTNB.

Data Analysis

All calculations were performed using the linear slope of the absorbance data obtained by the plate reader. Each slope had a coefficient of determination (R^2) value of 0.985 or greater unless the slope was significantly small. The outliers of the positive controls were then removed using the GraphPad outlier calculator (<https://www.graphpad.com/quickcalcs/grubbs1/>). The slopes from wells including either test compounds or the DMSO negative control were divided by the average of the positive control (either with BSA or without BSA) to determine the percent relative activity. These data were then transferred to GraphPad Prism 8 where experimental outliers were removed and the data were fit using a dose-response three- or four-parameter model comparison and the data were plotted.

Results

Solvent Dose-Response

The solvent dose-response assay showed significant precipitation (**Figure 12**). The wells containing pyridine showed the most precipitation followed by benzylamine. Triethylamine and cyclohexanone wells showed the least precipitation. The precipitates in pyridine and benzylamine wells developed in a bead formation at the bottom of the wells. The precipitates in the triethylamine and cyclohexanone wells essentially formed an opposite pattern, where the precipitate formed a ring around the outer edge of the well but not in the center where the solvent was added. The control wells, where an equal amount of phosphate buffer, distilled water, acetonitrile, or DMSO was added, did not show precipitation. Because of the significant amount of precipitation with the four solvents of interest, the activity data are not included.

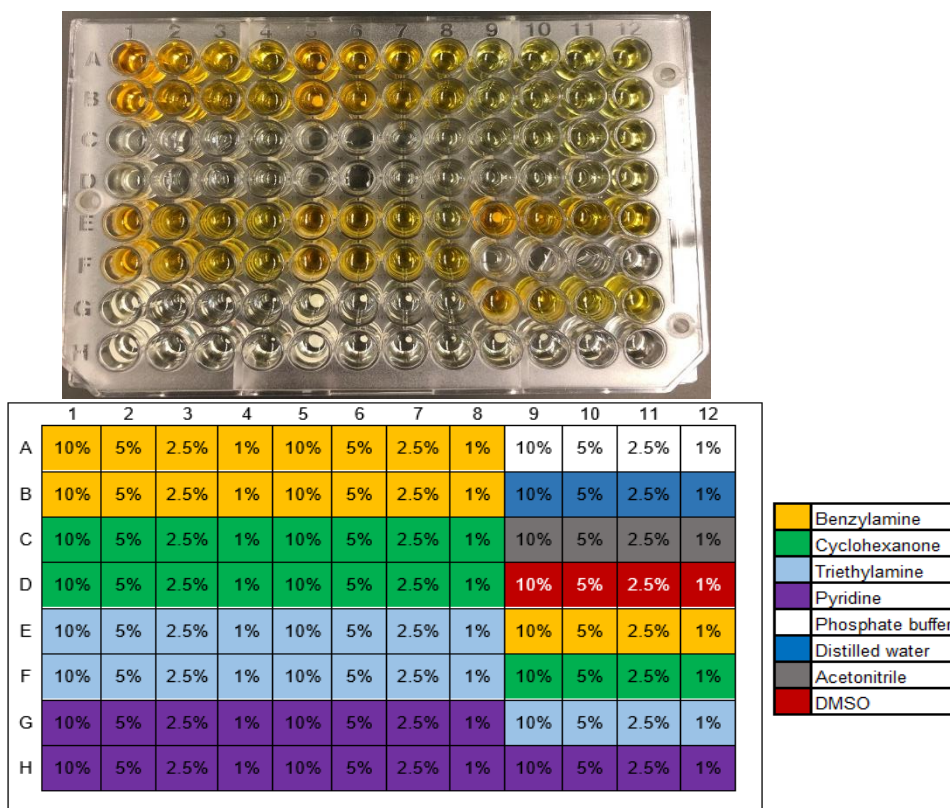


Figure 12: Precipitation (top) and plate map with concentrations (% v/v, bottom) from the solvent dose-response

Compound Dose-Response

As mentioned above, precipitation occurred during the first assay after the initial dilution despite sufficient mixing. Further, a precipitate was observed in the 3:1 acetone-DMSO negative control. Precipitation was also observed in all of the wells in the second assay including the 3:1 acetone-DMSO control.

Precipitation was absent in the third assay. However, only compounds **5** and **20** showed activity greater than the DMSO control (**Figure 13**). Compound **17** showed inhibition greater than that of DMSO. The activity data associated with compounds **6**, **10**, **19**, and **23** all converge on the DMSO data at the higher concentrations. The average activity of the positive control was 0.0017 $\mu\text{mol}/\text{min}$ with a coefficient of variation (CV) of 4%.

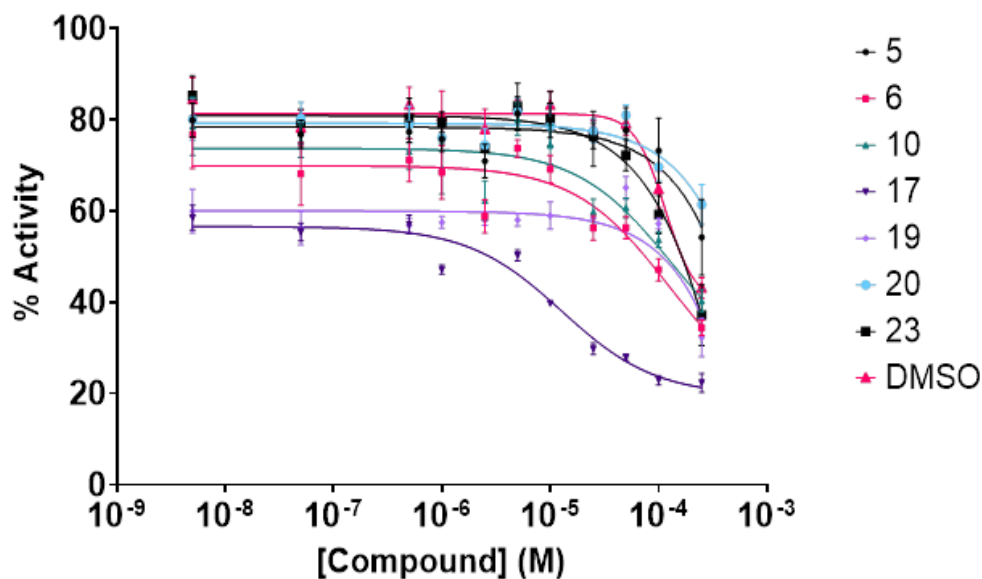


Figure 13: Results from the third assay

The results of the fourth assay were similar to the third assay. No precipitation was observed and only compounds **5** and **20** demonstrated activity greater than the DMSO control at

the highest concentration (**Figure 14**). However, compounds **20** and **23** showed activity greater than the DMSO control at 10 μ M. Compounds **17** and **19** showed similar inhibition of AChE. Compounds 6 and 10 showed activity in between DMSO and compounds **17** and **19**. The average activity of the positive control was 0.0017 μ mol/min with a CV of 2%.

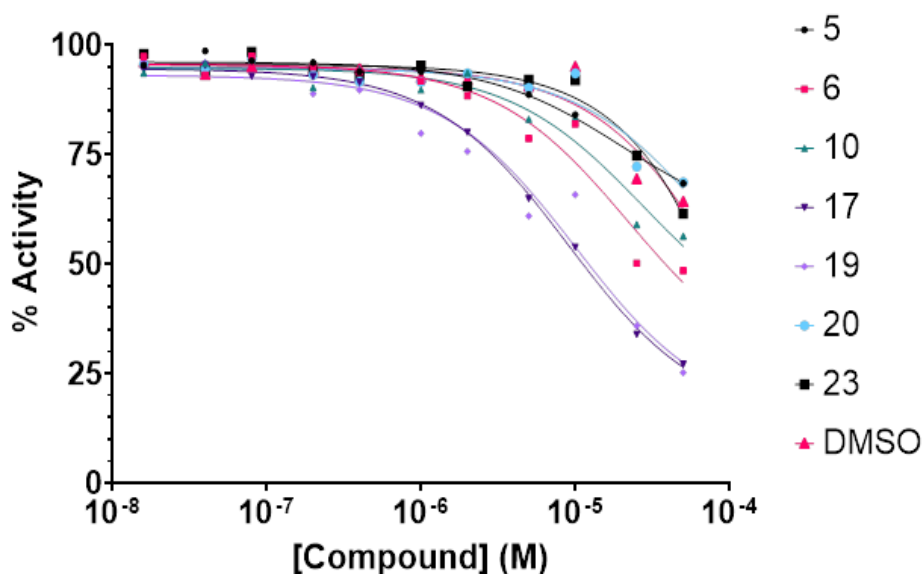


Figure 14: Results from the fourth assay

For the fifth assay, the A compounds demonstrated AChE inhibition greater than DMSO after the one-hour incubation (**Figure 15**). Both samples of **A4** showed almost complete

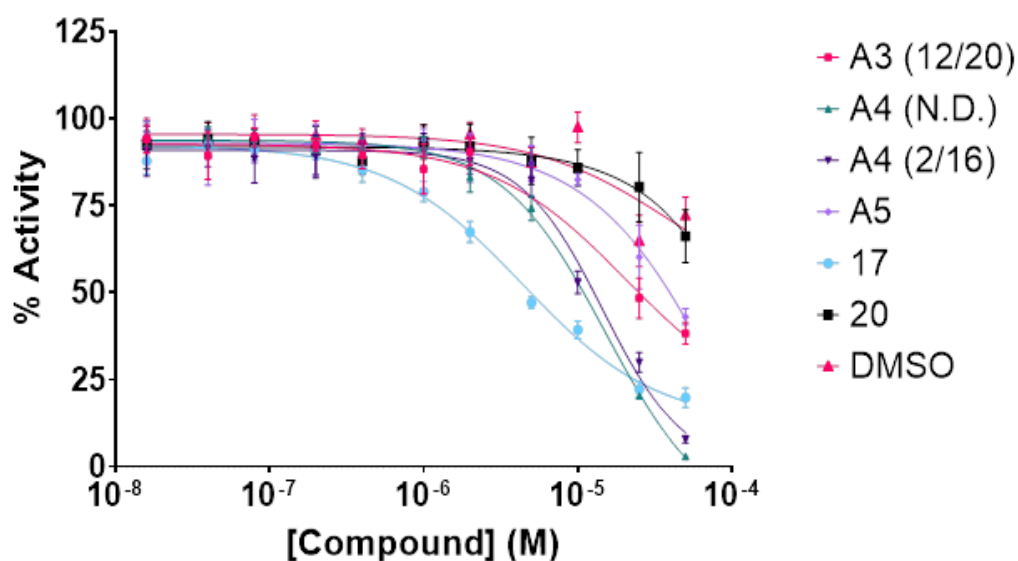


Figure 15: Results from the fifth assay (1-hour incubation)

inhibition at higher concentrations. **A3** and **A5** showed similar inhibition between the **A4** samples and DMSO. Compound **17** demonstrated a higher potency than the **A4** samples but did not achieve the same maximal inhibition. Compound **20** was similar to DMSO in this assay. The data after the two-hour incubation showed similar trends to the one-hour incubation (**Figure 16**). The average activity of the positive controls after the one-hour and two-hour incubation were both 0.0004 $\mu\text{mol}/\text{min}$ with a CV value of 5% for the one-hour incubation and a CV value of 4% for the two-hour incubation.

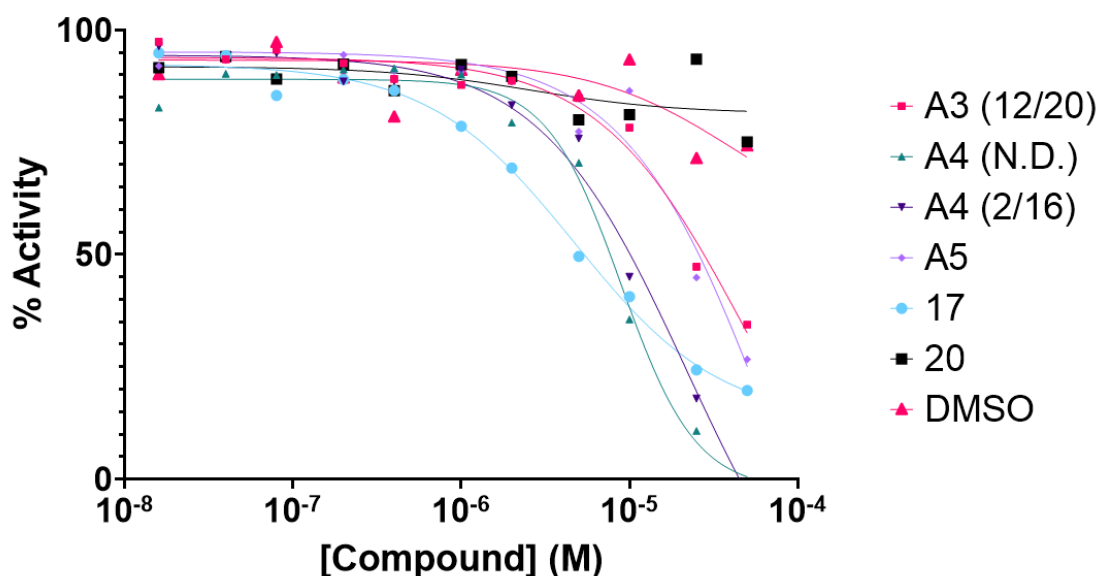


Figure 16: Results from the fifth assay (2-hour incubation)

The results of the sixth assay are nearly identical to the fifth assay (**Figure 17**). The average activity of the positive control for the sixth assay was 0.0004 $\mu\text{mol}/\text{min}$ with a CV of 2%.

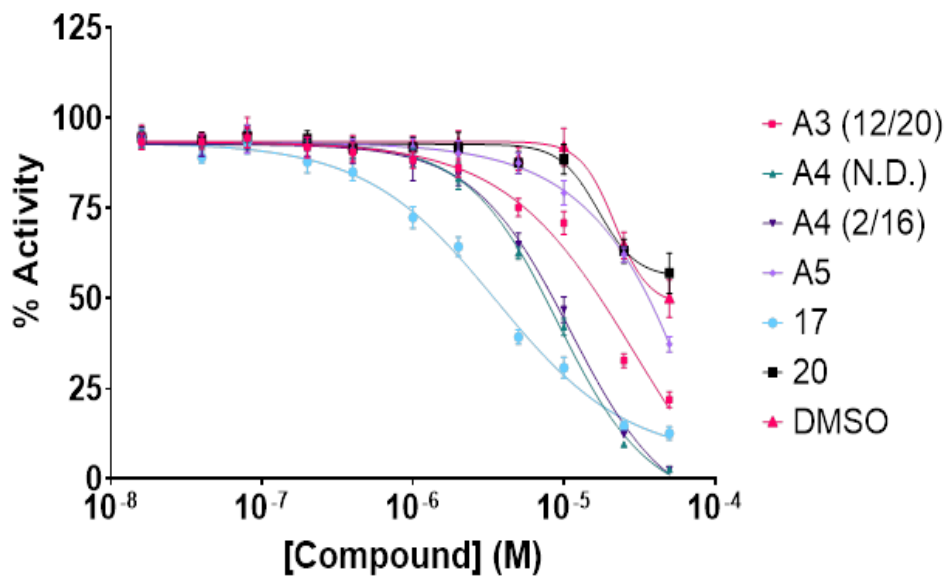


Figure 17: Results from the sixth assay

For the seventh assay, compounds **16**, **19**, **21**, and **25** demonstrated large increases in inhibition of AChE compared to DMSO (**Figures 18-21**). Compounds **1**, **2**, **3**, **4**, **6**, **8**, **10**, **11**, **15**, **18**, **22**, **24**, **26**, **27** showed modest increases in inhibition compared to DMSO. The data for compounds **5**, **7**, **9**, **12**, **13**, **14**, and **23**, as well as **A5** and 2-PAM, were similar to the DMSO control. The concentration of AChE in all four plates associated with the seventh assay yielded an activity of 0.0006 $\mu\text{mol}/\text{min}$ and CVs between 3% and 7%.

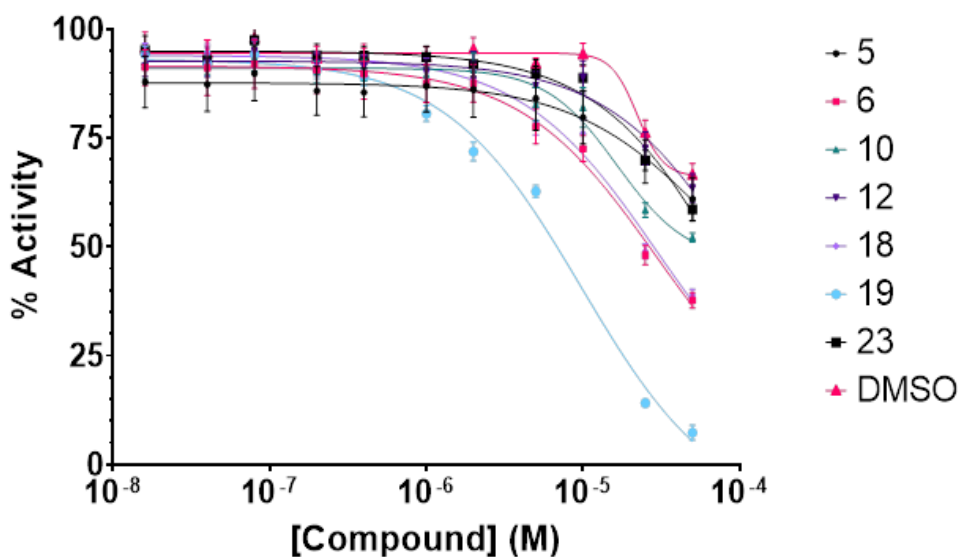


Figure 18: Results from the seventh assay (Part 1)

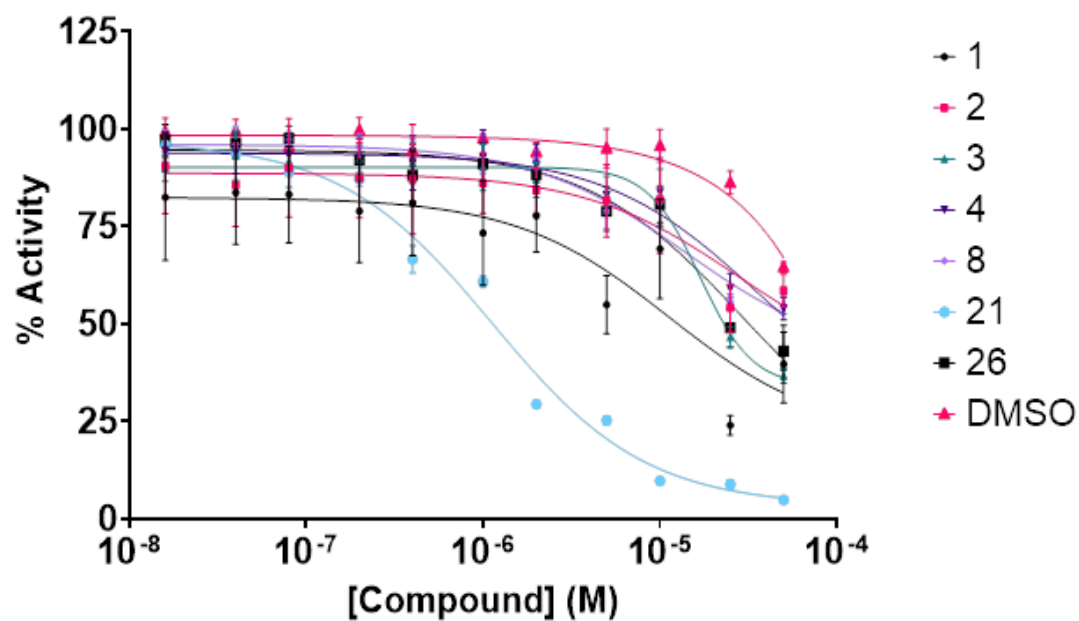


Figure 19: Results from the seventh assay (Part 2)

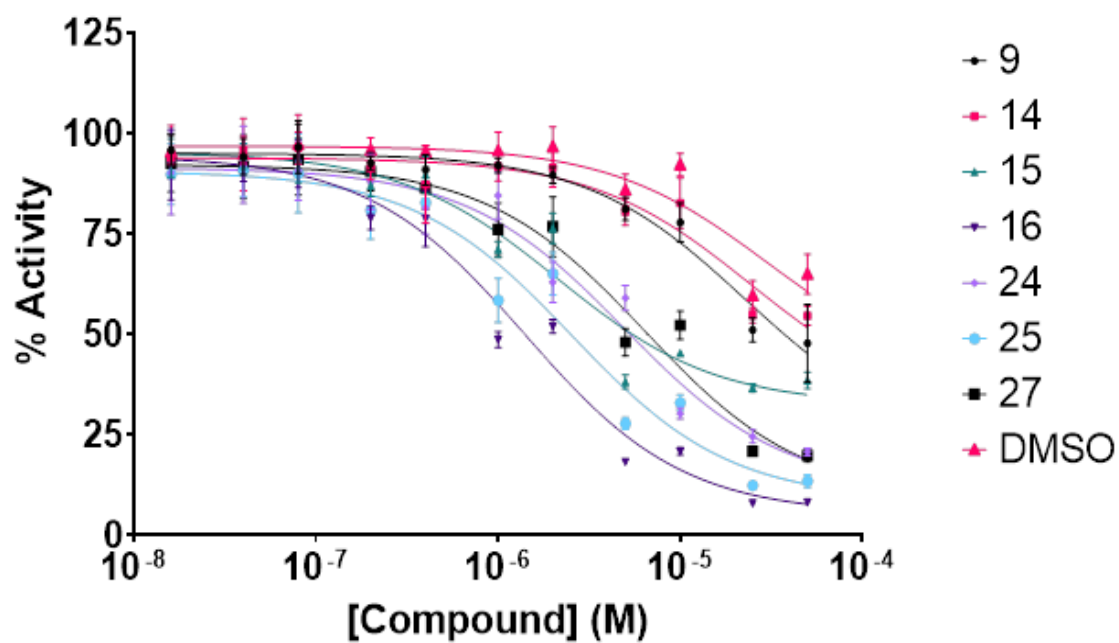


Figure 20: Results from the seventh assay (part 3)

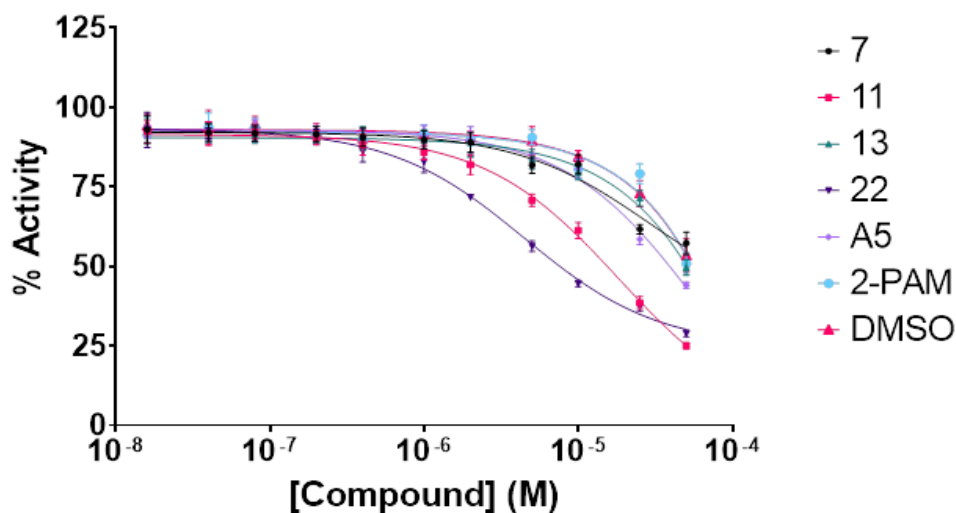


Figure 21: Results from the seventh assay (part 4)

For the eighth assay, compounds **11**, **15**, **16**, **17**, **19**, **22**, **24**, **25**, and **27** demonstrated large increases in inhibition of AChE compared to DMSO (**Figures 22-25**). Compounds **1**, **2**, **3**, **4**, **6**, **7**, **9**, **23**, **26**, **A3** (**12-20**), and **A5** showed modest increases in inhibition compared to DMSO. The data for compounds **10**, **12**, **13**, and **14** were similar to the DMSO control. There was a large amount of variation for compound **8**, and compound **18** lacked a clear trend. The concentration of AChE in both sets of corresponding positive controls yielded an activity of 0.0003 $\mu\text{mol}/\text{min}$ with CVs of 5% for plate 1 and 2% for plate 2.

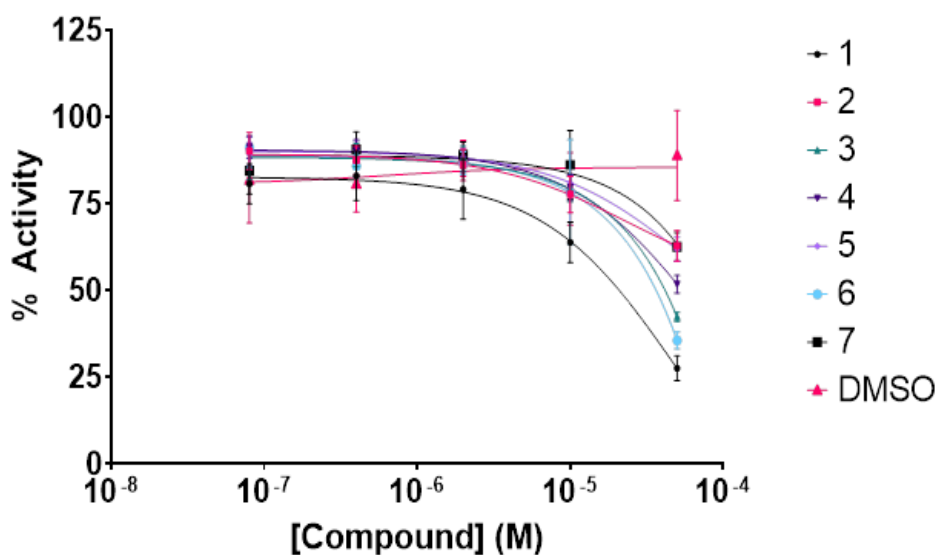


Figure 22: Results from the eighth assay (part 1)

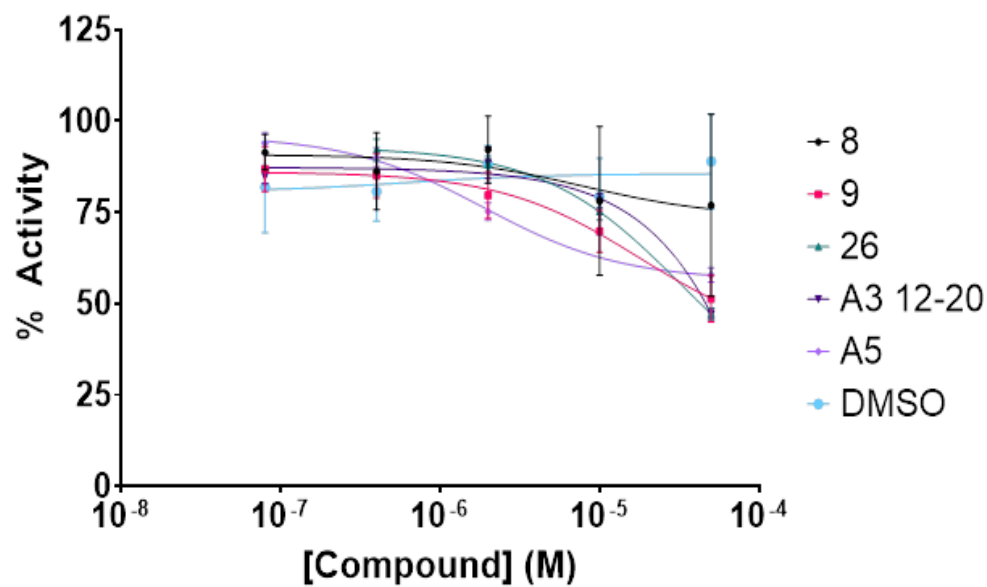


Figure 21: Results from the eighth assay (part 2)

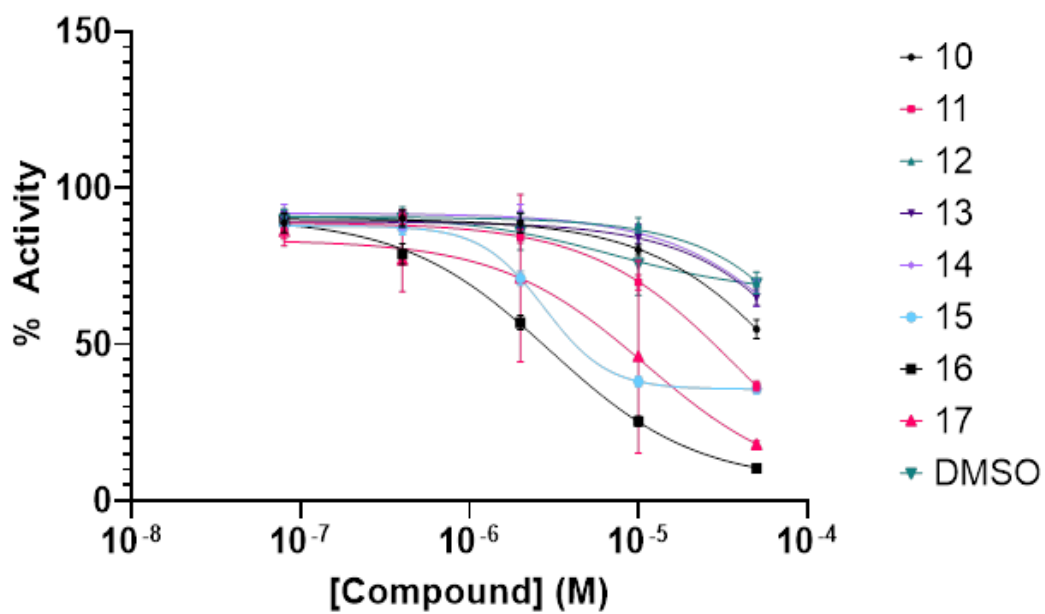


Figure 22: Results from the eighth assay (part 3)

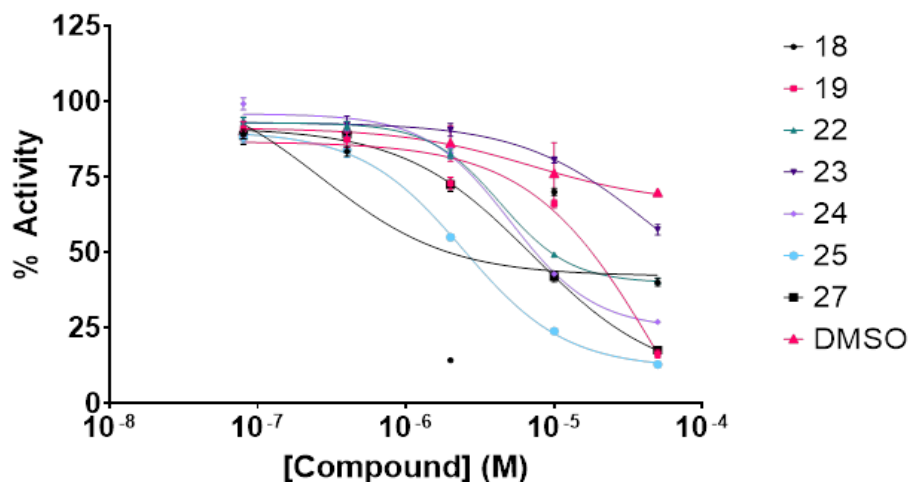


Figure 23: Results from the eighth assay (part 4)

For the ninth assay, compounds **16**, **17**, **19**, and **21**, as well as **A4 (2/16)**, demonstrated large increases in inhibition of AChE compared to DMSO (**Figures 26-29**). Compounds **1**, **6**, **7**, **8**, **11**, **15**, **18**, **20**, and **26**, as well as 2-PAM, doxepin, imipramine, chlorpromazine, trifluoperazine, and **A3 (12/20)**, showed modest increases in inhibition compared to DMSO. The data for compounds **2**, **3**, **4**, **5**, **9**, **12**, **13**, and **14** were similar to the DMSO control. There was a large amount of variation for compounds **10** and **A5** in addition to all four sets of DMSO controls. The concentration of AChE in both sets of corresponding positive controls yielded an activity of 0.0021 $\mu\text{mol}/\text{min}$ with CVs of 30% for plate 1 and 29% for plate 2.

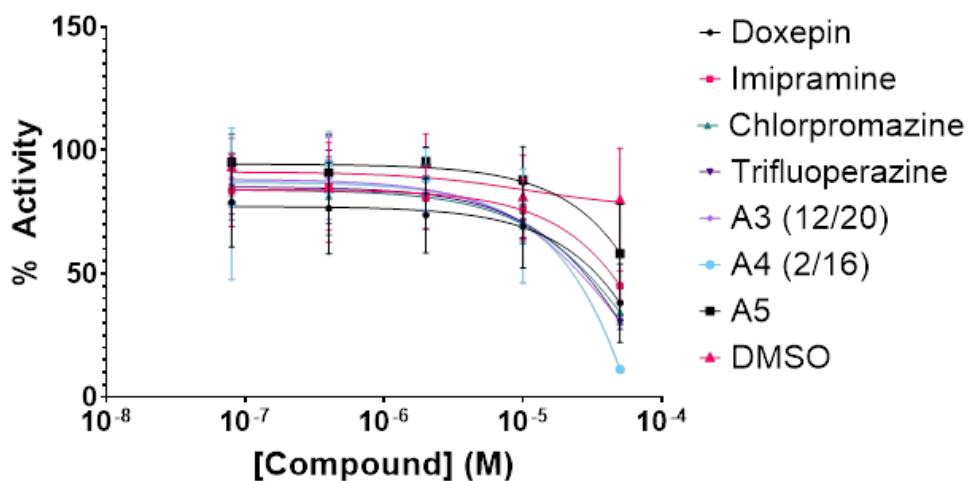


Figure 24: Results from the ninth assay (part 1)

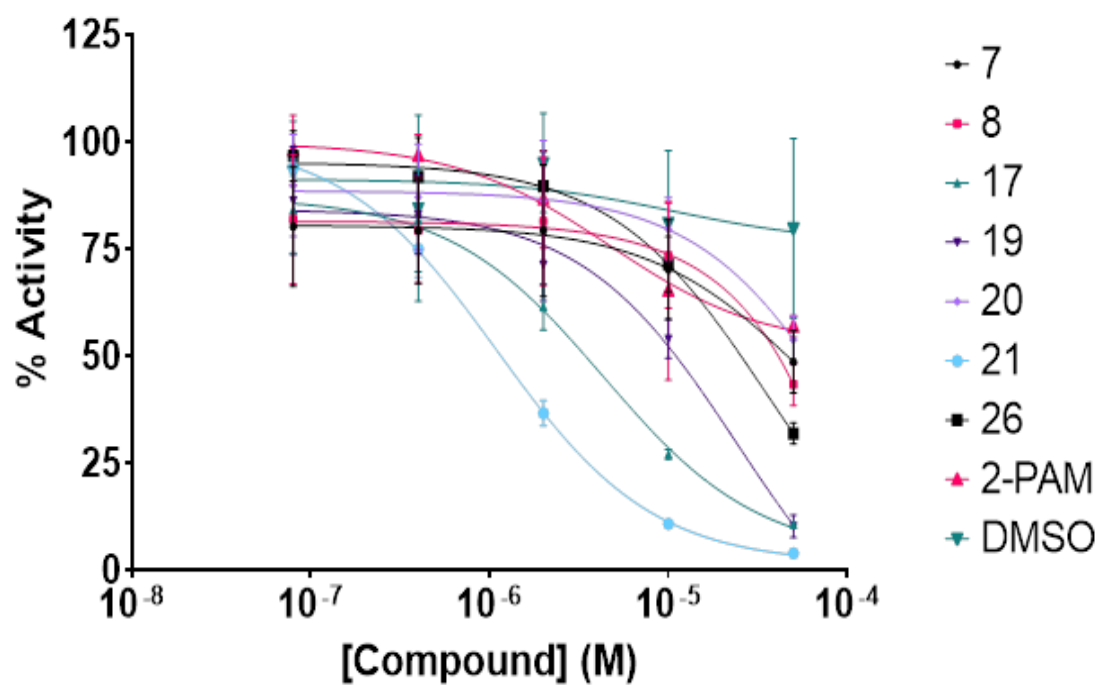


Figure 26: Results from the ninth assay (part 2)

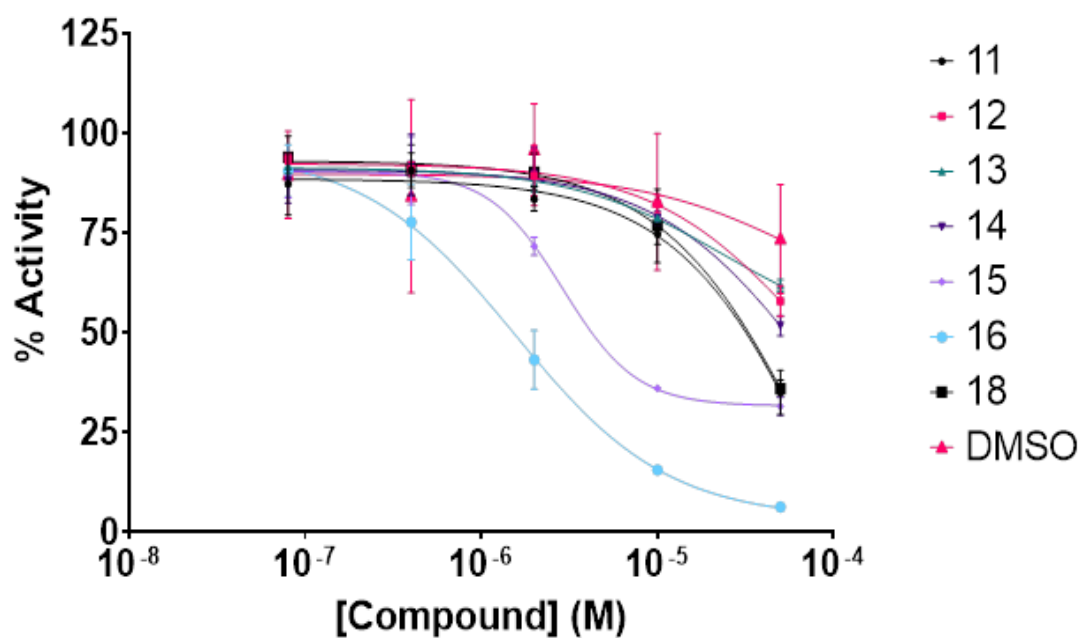


Figure 25: Results from the ninth assay (part 3)

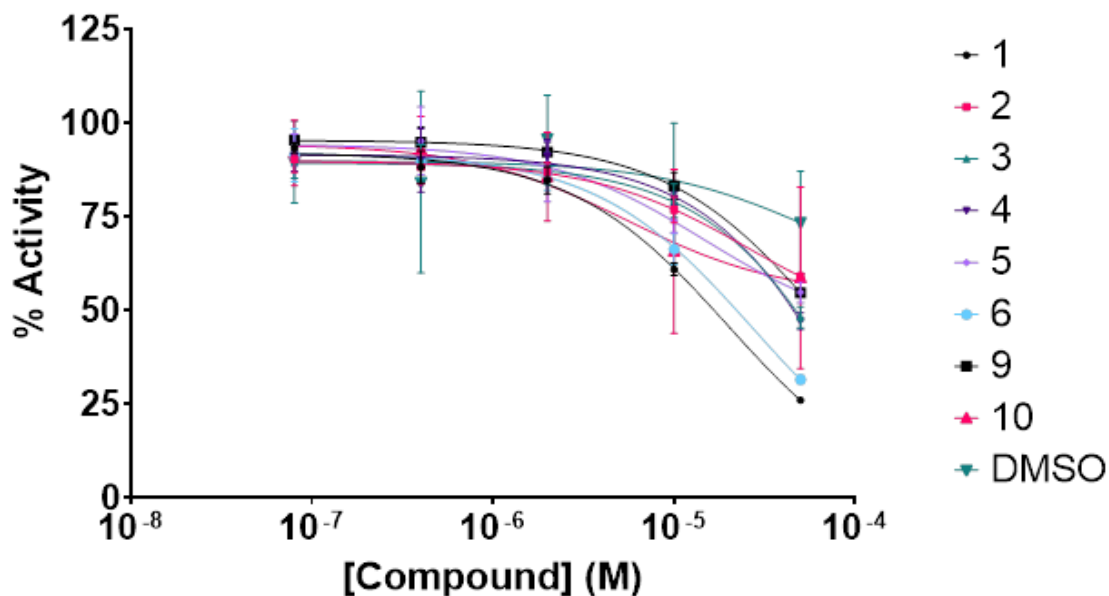


Figure 28: Results from the ninth assay (part 4)

For the tenth assay, compounds **16** and **21** demonstrated large increases in inhibition of AChE compared to DMSO (Figures 30-31). Compounds **7** and **8**, along with **A3** (12/20) and **A4** (N.D.), showed modest increases in inhibition compared to DMSO. The data for compounds **20**, **26**, **A5**, doxepin, imipramine, chlorpromazine, trifluoperazine, amitriptyline, and prochlorperazine were similar to the DMSO control. However, there was a large amount of variation associated with this assay. The concentration of AChE in the positive control including

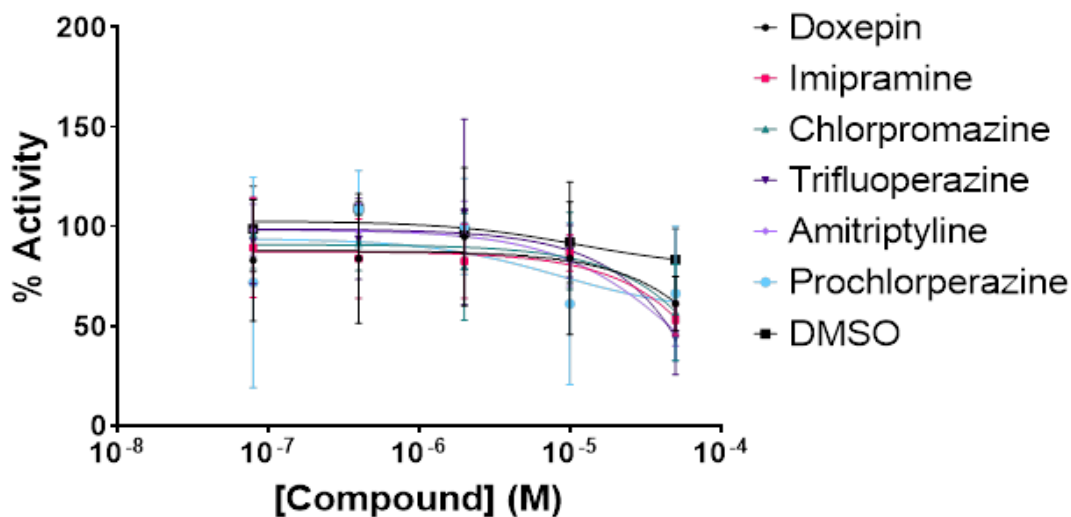


Figure 27: Results from the tenth assay (part 1)

BSA yielded an average activity of 0.0016 $\mu\text{mol}/\text{min}$ with a CV of 44%, whereas the positive control excluding BSA yielded an average activity of 0.0021 $\mu\text{mol}/\text{min}$ with a CV of 20%.

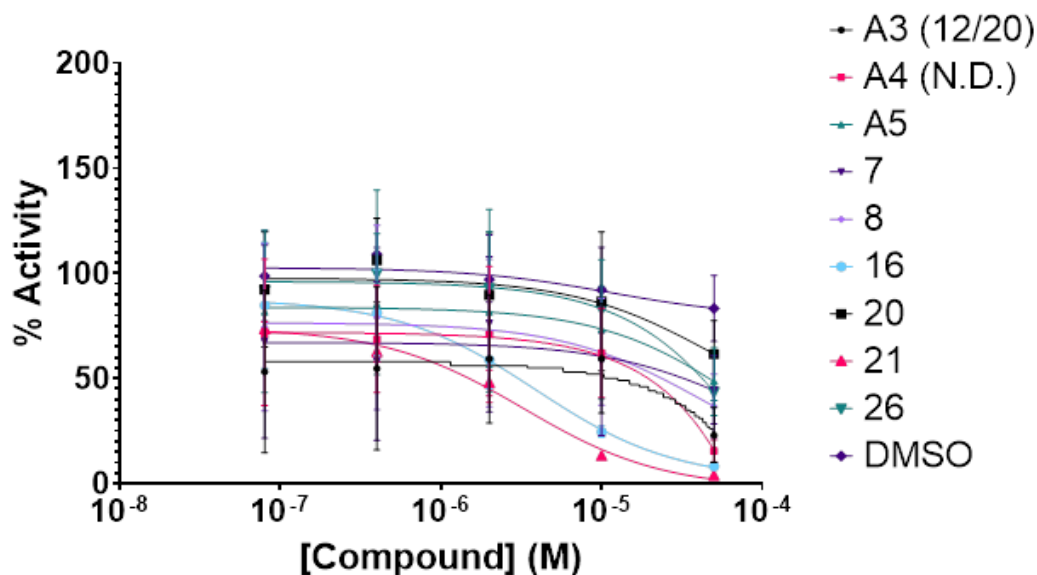


Figure 29: Results from the tenth assay (part 2)

Prior to the eleventh assay, the AChE stock solution stored in the fridge and the AChE incubated overnight showed over a 15-fold difference in activity with the former determined to have an average activity of 0.0114 $\mu\text{mol}/\text{min}$ and a CV of 26%, and the latter having an activity of 0.0007 $\mu\text{mol}/\text{min}$ with a CV value of 9%. The incubated AChE stock was then used for the eleventh assay. In the assay, compounds **7**, **8**, **16**, **20**, **21**, and **26**, as well as doxepin, imipramine, chlorpromazine, trifluoperazine, amitriptyline, **A3 (12/20)**, **A4 (N.D.)**, and **A5** demonstrated inhibition of AChE greater than that of DMSO (**Figures 32-33**). Prochlorperazine showed an increase in activity at the highest concentration above the DMSO control but was within one standard deviation of the DMSO control. However, there was a large amount of variation associated with this assay. The concentration of AChE in the positive control including BSA

yielded an average activity of 0.0016 $\mu\text{mol}/\text{min}$ with a CV of 44%, whereas the positive control excluding BSA yielded an average activity of 0.0021 $\mu\text{mol}/\text{min}$ with a CV of 20%.

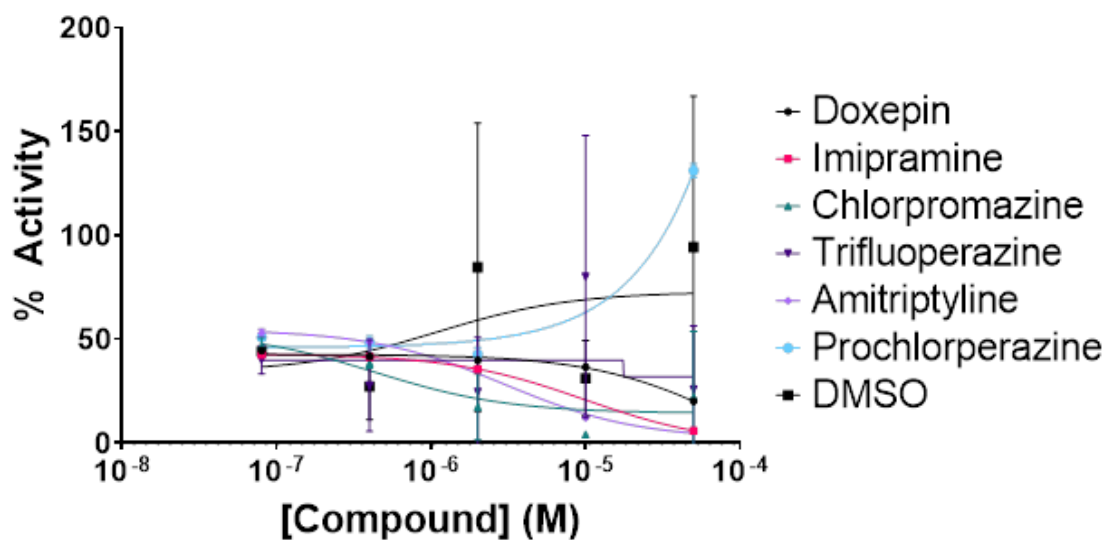


Figure 30: Results from the 11th assay (part 1)

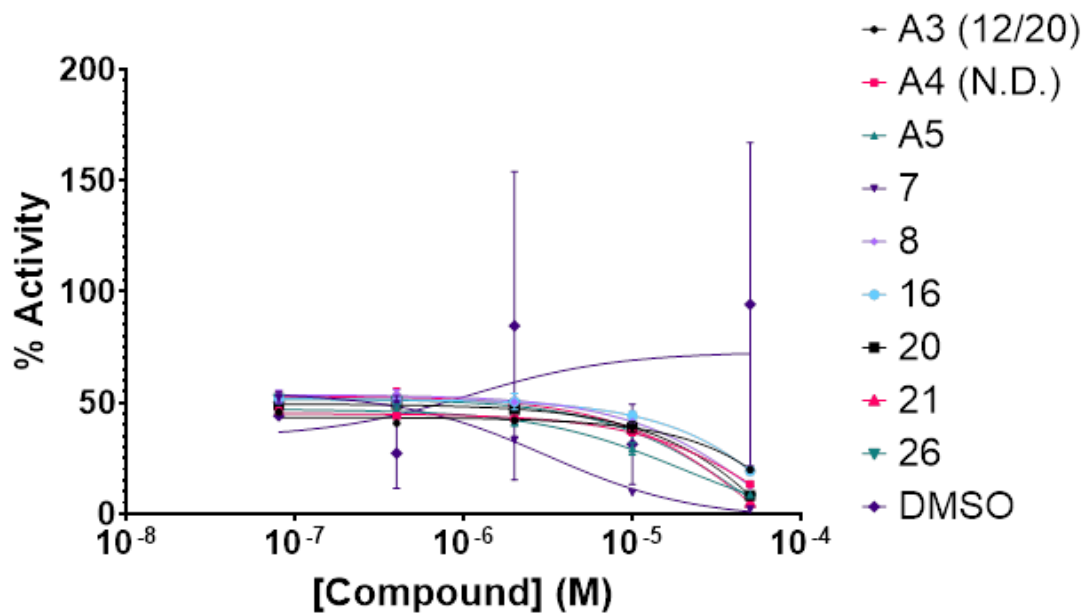


Figure 31: Results from the 11th assay (part 2)

Single-Point Test

For the single-point assays, several compounds showed greater activity than the DMSO control. 2-PAM, compound **20**, **A5**, and **A4 (2/16)** showed the greatest increases for the 125-uM experiment (**Figure 34**). For the 250-uM experiment, only compounds **13** and **20** yielded activity above the DMSO control average with both being within one standard deviation of the DMSO average (**Figure 35**). However, precipitation was observed in most of the wells from both experiments including the wells with compounds **13**, **20**, **A4 (2/16)**, and **A5** (**Figure 36**). The activities of AChE in the positive controls for the 125-uM and 250-uM experiments were 0.0405 umol/min and 0.0415 umol/min, respectively.

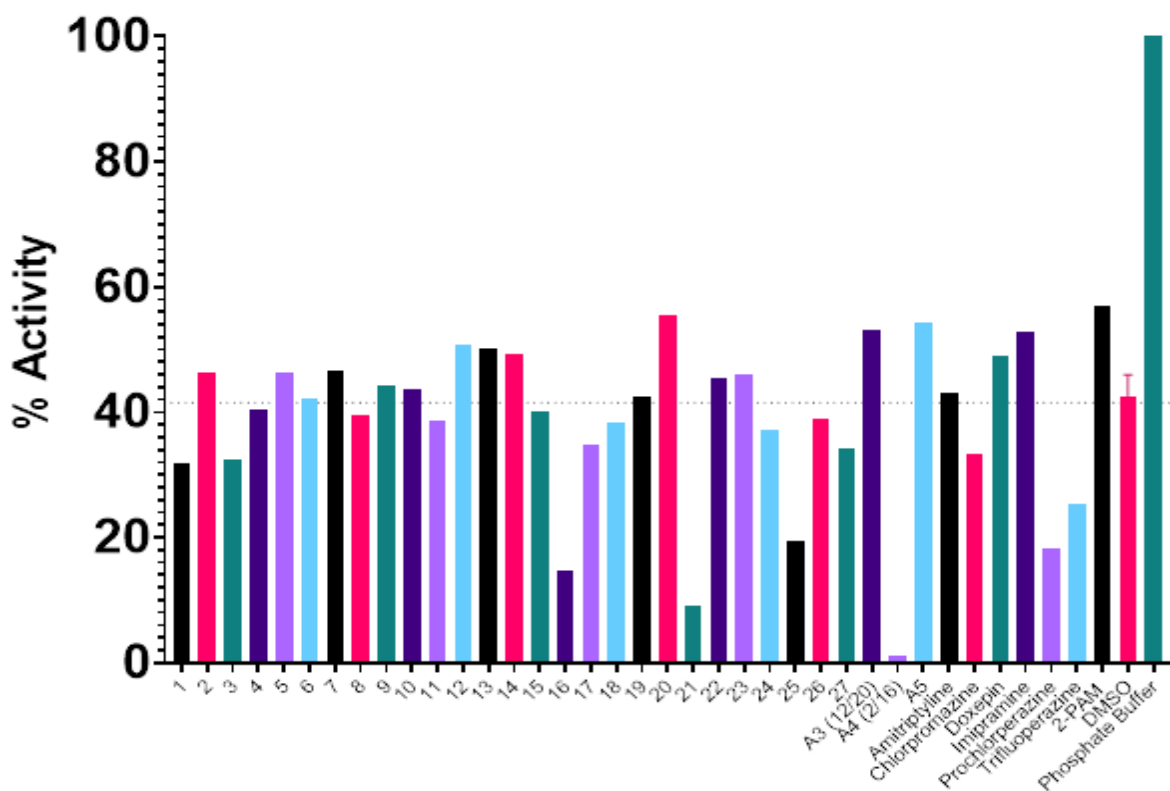


Figure 32: Results from the 125-uM single-point assay

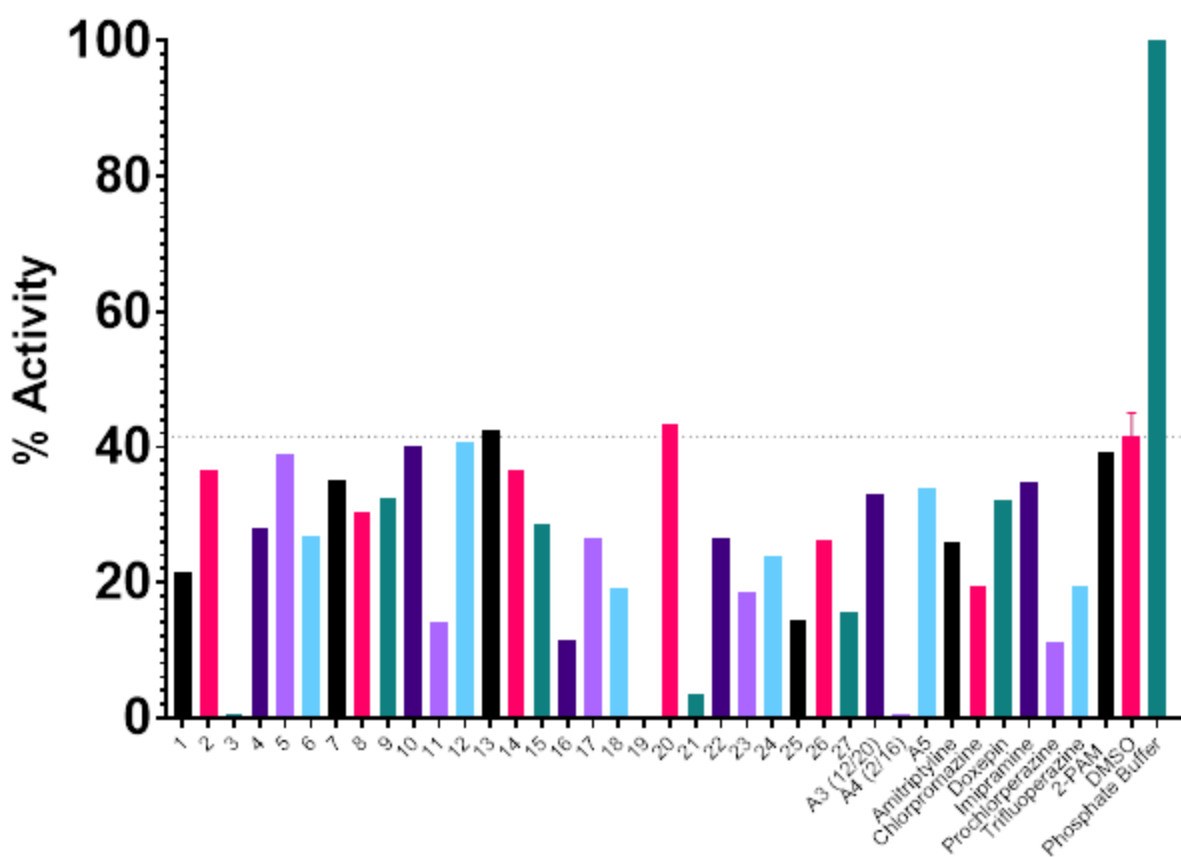
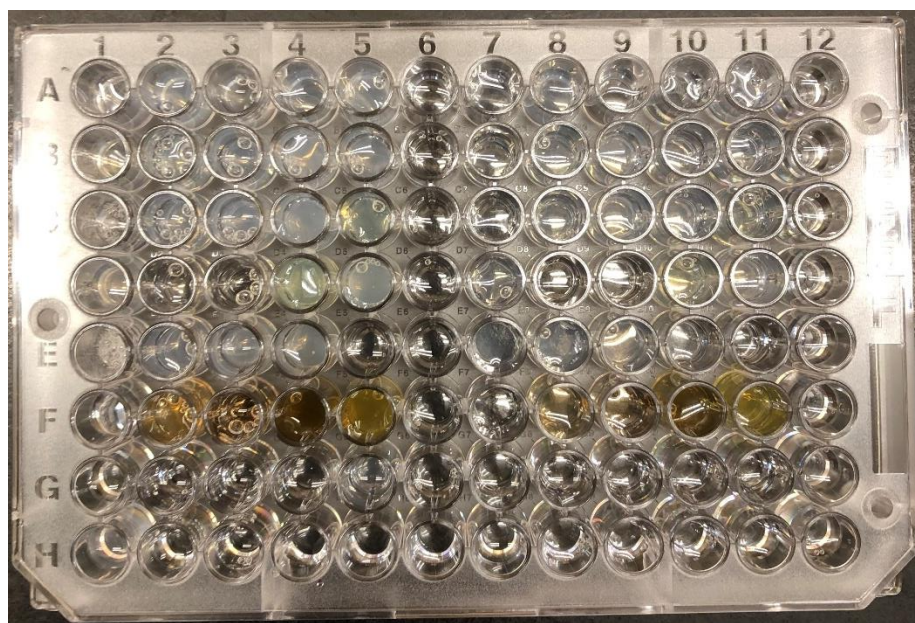


Figure 33: Results from the 250-uM single-point assay



	1	2	3	4	5	6	7	8	9	10	11	12
A	1	2	3	4	5	DMSO	1	2	3	4	5	DMSO
B	6	7	8	9	10	DMSO	6	7	8	9	10	DMSO
C	11	12	13	14	15	DMSO	11	12	13	14	15	DMSO
D	16	17	18	19	20	DMSO	16	17	18	19	20	DMSO
E	21	22	23	24	25	DMSO	21	22	23	24	25	DMSO
F	26	27	A3	A4	A5	DMSO	26	27	A3	A4	A5	DMSO
G	Amitriptyline	Chlorpromazine	Doxepin	Imipramine	Prochlorperazine	DMSO	Amitriptyline	Chlorpromazine	Doxepin	Imipramine	Prochlorperazine	DMSO
H	Trifluoperazine	2-PAM	PB	PB	PB	DMSO	Trifluoperazine	2-PAM	PB	PB	PB	DMSO

Figure 34: Precipitation (top) and plate map (bottom) from single-point assays with the 250-uM experiment in columns 1-6 and the 125-uM experiment in columns 7-12

Discussion

In the solvent dose-response assay, several organic solvents resulted in the formation of precipitates. At first, this was surprising because of the absence of compound. However, upon further investigation, it was discovered that BSA has low solubilities in most organic solvents that are not polar protic (Houen, 1996). This is fairly consistent with the amount of precipitate formation seen in the solvent dose-response assay. First, the amount of precipitate seen with triethylamine, cyclohexanone, benzylamine, and pyridine correlated with polarity. Triethylamine and cyclohexanone had approximately the least precipitate formation and are the most polar. Benzylamine resulted in more precipitation but is less polar since the amine group is connected to a nonpolar benzene ring. Pyridine, a polar aprotic solvent, resulted in the most precipitation. Interestingly, despite DMSO being polar aprotic, BSA was shown to have a relatively high solubility in DMSO (Houen, 1996) which is likely why no precipitate formed in the DMSO wells. However, acetone is a polar aprotic solvent which could explain the formation of precipitate in the 3:1 acetone-DMSO negative controls seen in the dose-response assays and the absence of precipitate in the DMSO only wells (**Figure 12**).

The first compound dose-response assay procedure could not be completed as the first dilution resulted in a precipitate and the concentration in the remaining wells of the plate required that the previous concentration in the dilution series be precise and accurate. Because precipitation was observed, it was obvious that the concentration could not be precisely or accurately calculated. To better account for possible precipitation, the modification of the first assay to the second assay was to introduce new direct dilutions so that if precipitation were to occur in higher concentration wells, there would be other wells in the plate with concentrations

that would remain unaffected. Unfortunately, as mentioned above, precipitation was observed in all three initial dilution columns even in the second assay.

Because none of the direct dilutions were successful in the second assay, and the literature EC₅₀ values are sufficiently low, the final compound concentrations used in the third assay were decreased. Additionally, all of the compounds were prepared at 10 mM in DMSO prior to this assay. These changes led to the complete elimination of observable precipitation at the concentrations used. However, the third assay showed only two compounds that resulted in activities greater than the DMSO control, but the differences were marginal compared to literature values for similar compounds (**Figure 13**).

Considering the solubility issues in dissolving the compounds to make stock solutions in the first and second assays, the third assay procedure was modified to include the droplet method, similar to Chapleau et al. (2015), and was used for the fourth assay. Similar to the results of the third assay, the fourth assay yielded only marginal increases in activity above the DMSO control (**Figure 14**). Solubility was still a concern, so the incubation time was adjusted to one and two hours for the fifth assay to allow more time for the compounds to dissolve in case they were not completely solubilized. The **A** compounds were also included so that a direct comparison the Chapleau et al. (2015) experiments could be made. However, the data for the one-hour and two-hours incubations were still similar to the data from the fourth assay (**Figures 15-16**). Considering that the incubation times for the Chapleau et al. (2015) and Katz et al. (2018) experiments were 10 minutes and 15 minutes respectively, a one-hour incubation should have been more than sufficient to produce the desired results. For this reason, only a one-hour incubation was performed for the sixth through eleventh dose-response assays, as well as the single-point assays.

For the sixth assay, the 200 mM sodium phosphate buffer was replaced with 40 mM sodium phosphate buffer to determine if the ionic strength of the solution impacted the interactions between the compounds and AChE. The fifth assay procedure was then repeated with this change to provide a direct comparison. However, the change in ionic strength did not appear to affect the results as the data from the fifth and sixth assays are nearly identical (**Figures 15 & 17**).

The seventh assay was a repeat of the procedure for the fifth assay with different compounds and a slightly higher final concentration of AChE. Because it seemed that all of the compounds were completely solvated, other compounds were also tested to determine if they activated AChE. Unfortunately, this was not the case as all of the data associated with the compounds showed either inhibition similar to DMSO or inhibition greater than DMSO (**Figure 18-21**). The seventh assay procedure was then modified to include more compounds (15 compounds plus the DMSO control vs the 7 compounds and DMSO control in the previous procedure) because the lower concentrations were not showing a significant difference in activity compared to DMSO. This allowed the compounds to be screened more quickly and efficiently.

As mentioned above, the 300 uL Voyager pipette could no longer be used as the tips were depleted but instead had to be swapped with the 1250 uL pipette for the ninth through eleventh assays due to shipping delays related to the COVID-19 pandemic. This was not ideal as the volumes being pipetted were on the lower end of the 1250 uL pipette range. The change to the 1250 uL pipette had a significant impact as the coefficient of variation (CV) for the ninth through eleventh assays was significantly greater (20-44%) compared to the previous assays (2-11%) which did not use the 1250 uL pipette. It is likely that this variation resulted because the volumes that were dispensed were on the lower end of the pipetting range for the 1250 uL pipette. The

error by the pipette would have then been exacerbated with each serial dilution (Hanson et al., 2015). Further, despite the DMSO control being prepared in parallel with the compounds, the data for DMSO showed significant variation (**Figures 26-33**). Additionally, for the ninth assay, the concentration of AChE was increased. The thought was that at higher concentrations a greater fraction of the enzyme would be a dimer since AChE is known to dimerize (Sakayanathan et al., 2019). However, the results were largely the same from the previous assays meaning it is unclear whether the enzyme had a different globular form compared to the previous assays, or whether the compounds have the same effect on the monomer as the dimer.

When the results obtained in the previous assays failed to reproduce those in the literature, the methods of Chapleau et al. (2015) and Katz et al. (2018) were analyzed again, and it was noted that BSA was not included in their procedures. Therefore, the ninth dose-response assay procedure was modified for the tenth assay to exclude BSA. In fact, one possible explanation for the discrepancy is that the compounds used by Chapleau et al. (2015) and Katz et al. (2018) did not actually activate AChE but rather stabilized AChE or refolded denatured or misfolded enzyme. BSA is known to stabilize AChE (Estrada-Mondaca & Fournier, 1998) and bind drugs with different structural motifs (Wani et al., 2021; Coura et al., 2021). The thought was that by excluding BSA, if the test compounds were stabilizing AChE, then this effect might not be as noticeable if BSA was stabilizing the positive control, or if BSA was binding the compounds leaving less compound available to bind to AChE. It is also possible that the mechanism by which BSA stabilizes AChE actually prevents the binding of the test compounds. In the controls for the Chapleau et al. (2015) and Katz et al. (2018) experiments, where the compounds were not present, the amount of remaining active AChE may have decreased while the AChE activity in the test solutions remained the same giving the appearance that the

compounds activated AChE. Alternatively, the compounds could have helped to refold denatured or misfolded enzyme, and despite the constant relative activity in the controls, the amount of activity in the test wells would have appeared to increase without actually activating AChE. However, neither the tenth assay nor the eleventh assay demonstrated results similar to either the Chapleau et al. (2015) or Katz et al. (2018) experiments (**Figures 30-33**). Both assays excluded BSA, and the AChE for the eleventh assay was incubated at pH 6.0 and 37°C to test the refolding hypothesis. The activity of the incubated AChE versus nonincubated AChE did show a large difference suggesting that AChE was, in fact, denatured by the incubation process.

The single-point tests excluded BSA but still resulted in precipitation for both 250 uM and 125 uM concentrations (**Figures 36**). If the solvent, DMSO, was precipitating AChE, similar to what was observed with BSA in the solvent-dose response assay, then it would be expected that precipitation should also occur in the DMSO control wells. However, no precipitation was observed in the DMSO control wells at either 2.5% or 1.25% DMSO. Additionally, the amount of precipitation across multiple assays positively correlated with the volume of test compound solution that was dispensed. The data from the single-point assays also did not show increases in activity comparable to that seen in the Chapleau et al. (2015) and Katz et al. (2018) experiments (**Figures 34-35**).

Therefore, none of the results that were obtained are consistent with the results from the literature. Only a few compounds showed slight increases above the negative DMSO controls in the dose-response assays. In fact, some of the compounds demonstrated strong inhibition of AChE including the A compounds and the FDA-approved drugs. This is in sharp contrast to the multi-fold increases in activity that were reported previously. In particular, **A3**, **A4**, and **A5** had EC₅₀ values of less than 10 uM in human AChE (Chapleau et al., 2015) but were observed here

as either showing no change in activity or showing inhibition. Several explanations could be provided to give rationality to the discrepancies.

One possible explanation for the discrepancies has to do with the specialized pipette tips that were being used during this project. The Low Retention pipette tips are made of a polypropylene blend that have heightened hydrophobic properties according to Integra's website (<https://www.integra-biosciences.com/united-states/en/pipette-tips>). Although polypropylene is largely insoluble, the hydrophobic properties could affect nonpolar solvents and solutions. Integra has stated this may affect volume measurements of more nonpolar solutions, but there is also a possibility this could draw nonpolar solutes out of solution. Considering the compounds would not dissolve in more polar solvents (**Table 1**), these Low Retention tips may have interacted with the compounds.

Another possible explanation for the discrepancy in results, is that the isoform and globular form of AChE that was used may have varied between experiments. The Chapleau et al. (2015) experiments used one of two forms of human AChE or mouse AChE. Interestingly, the mouse AChE showed greater affinity for the compounds than the human AChE (Chapleau et al., 2015). Because the Katz et al. (2018) experiments used monomeric mouse AChE and the Radic AChE most closely resembles dimeric human AChE, it is possible the structural differences had an impact on the FDA-approved drugs activating AChE. Further, differences between the human AChE used in the Chapleau et al. (2015) experiments and the Radic isoform may also explain the differences with those results. However ultimately, the exact effect of structural variations between AChE isoforms on interactions with the test compounds is unknown.

The last possible reason for the discrepancy in results that will be detailed here relates to the storage of the solubilized compounds. After each compound was prepared in solution, they

were stored at -80°C until they were ready for use, at which time they would be removed and allowed to slowly come to room temperature. Again, solubility was an issue so the compounds were mixed on either the Benchmark BV1010 Multi-tube Vortexer or an Eppendorf Thermomixer. The friction on the vortexer was sufficient to heat the tubes, but if the compounds were placed on the Thermomixer, the temperature was set to 37°C. With the large number of experiments performed, there is a possibility that the freeze/thaw cycles impacted the structural integrity of the compounds (Kozikowski et al., 2003). Further, the **A** compounds provided by Dr. McElroy were the result of decomposition from other compounds (McElroy, 2019), so it would be unsurprising if any of the **A** compounds or compounds **1-27** degraded in addition to any structural changes from the freeze/thaw cycles.

Regardless of the cause, the inability to reproduce the literature values across multiple assays provides a valid reason to question the data from Chapleau et al. (2015) and Katz et al. (2018). With the current data, it is difficult to say whether the literature trends or the trends presented in this paper are more accurate. A fairly obvious step towards validating the data presented from this project would be to verify the structures of each compound by NMR. Additionally, as it is possible that the denaturing procedure did not truly mimic the denaturing or misfolding process that might have occurred in the AChE used in the Chapleau et al. (2015) and Katz et al. (2018) experiments, designing a set of procedures with varying conditions to denature or misfold the AChE could help elucidate the cause of the discrepancies. Lastly, a substrate concentration of 0.5 mM was used consistently with every assay that was performed in this project. However, Chapleau et al. (2015) and Katz et al. (2018) noted the use of a final concentration of ATC at 1 mM and 2 mM, respectively. Therefore, it may be worthwhile to

perform an assay procedure that includes varied ATC concentrations alongside the compounds to determine if the substrate concentration effects the results.

References

- Alvarez, A., Alarcón, R., Opazo, C., Campos, E. O., Muñoz, F. J., Calderón, F. H., Dajas, F., Gentry, M. K., Doctor, B. P., De Mello, F. G., & Inestrosa, N. C. (1998). Stable complexes involving acetylcholinesterase and amyloid-beta peptide change the biochemical properties of the enzyme and increase the neurotoxicity of Alzheimer's fibrils. *J Neurosci*, 18(9), 3213-3223.
- Atwood, D., Paisley-Jones, C. (2017). *Pesticides Industry Sales and Usage: 2008-2012 Market Estimates*.
- Chapleau, R. R., McElroy, C. A., Ruark, C. D., Fleming, E. J., Ghering, A. B., Schlager, J. J., Poeppelman, L. D., & Gearhart, J. M. (2015). High-Throughput Screening for Positive Allosteric Modulators Identified Potential Therapeutics against Acetylcholinesterase Inhibition. *J Biomol Screen*, 20(9), 1142-1149. <https://doi.org/10.1177/1087057115591006>
- Colović, M. B., Krstić, D. Z., Lazarević-Pašti, T. D., Bondžić, A. M., & Vasić, V. M. (2013). Acetylcholinesterase inhibitors: pharmacology and toxicology. *Curr Neuropharmacol*, 11(3), 315-335. <https://doi.org/10.2174/1570159X11311030006>
- Coura, C. P. M., Fragoso, V. M. D. S., Valdez, E. C. N., Paulino, E. T., Silva, D., & Cortez, C. M. (2021). Study on the interaction of three classical drugs used in psychiatry in albumin through spectrofluorimetric modeling. *Spectrochim Acta A Mol Biomol Spectrosc*, 255, 119638. <https://doi.org/10.1016/j.saa.2021.119638>
- Estrada-Mondaca, S., & Fournier, D. (1998). Stabilization of recombinant Drosophila acetylcholinesterase. *Protein Expr Purif*, 12(2), 166-172. <https://doi.org/10.1006/prep.1997.0831>
- Franjesevic, A. J., Sillart, S. B., Beck, J. M., Vyas, S., Callam, C. S., & Hadad, C. M. (2019). Resurrection and Reactivation of Acetylcholinesterase and Butyrylcholinesterase. *Chemistry*, 25(21), 5337-5371. <https://doi.org/10.1002/chem.201805075>
- Grifman, M., Arbel, A., Ginzberg, D., Glick, D., Elgavish, S., Shaanan, B., & Soreq, H. (1997). In vitro phosphorylation of acetylcholinesterase at non-consensus protein kinase A sites enhances the rate of acetylcholine hydrolysis. *Brain Res Mol Brain Res*, 51(1-2), 179-187. [https://doi.org/10.1016/s0169-328x\(97\)00246-5](https://doi.org/10.1016/s0169-328x(97)00246-5)
- Gupta, R. C. (2015). *Handbook of toxicology of chemical warfare agents* (Second ed.). Academic Press.
- Gupta, R. C. (2020). *Handbook of toxicology of chemical warfare agents* (Third ed.). Academic Press.

- Hanson, S. M., Ekins, S., & Chodera, J. D. (2015). Modeling error in experimental assays using the bootstrap principle: understanding discrepancies between assays using different dispensing technologies. *J Comput Aided Mol Des*, 29(12), 1073-1086. <https://doi.org/10.1007/s10822-015-9888-6>
- Houen, G. (1996). The solubility of proteins in organic solvents. 50, 68-70. <https://doi.org/10.3891/acta.chem.scand.50-0068>
- Katz, F. S., Pecic, S., Schneider, L., Zhu, Z., Hastings-Robinson, A., Luzac, M., Macdonald, J., Landry, D. W., & Stojanovic, M. N. (2018). New therapeutic approaches and novel alternatives for organophosphate toxicity. *Toxicol Lett*, 291, 1-10. <https://doi.org/10.1016/j.toxlet.2018.03.028>
- Kozikowski, B. A., Burt, T. M., Tirey, D. A., Williams, L. E., Kuzmak, B. R., Stanton, D. T., Morand, K. L., & Nelson, S. L. (2003). The effect of freeze/thaw cycles on the stability of compounds in DMSO. *J Biomol Screen*, 8(2), 210-215. <https://doi.org/10.1177/1087057103252618>
- Kumar, A., & Darreh-Shori, T. (2017). DMSO: A Mixed-Competitive Inhibitor of Human Acetylcholinesterase. *ACS Chem Neurosci*, 8(12), 2618-2625. <https://doi.org/10.1021/acscchemneuro.7b00344>
- McElroy, C. A. (2019). *Making the Fastest Faster: Positive Allosteric Modulation of Acetylcholinesterase for the Treatment of OP Poisoning* [PowerPoint].
- Meriney, S. D., Fanselow, E. E., & Ebook Central Academic, C. (2019). *Synaptic transmission*. Academic Press.
- Michel, H. O., & Krop, S. (1951). The reaction of cholinesterase with diisopropyl fluorophosphate. *J Biol Chem*, 190(1), 119-125.
- Peter, J. V., Sudarsan, T. I., & Moran, J. L. (2014). Clinical features of organophosphate poisoning: A review of different classification systems and approaches. *Indian J Crit Care Med*, 18(11), 735-745. <https://doi.org/10.4103/0972-5229.144017>
- Reiner, E., & Simeon-Rudolf, V. (2000). Cholinesterase: substrate inhibition and substrate activation. *Pflugers Arch*, 440(Suppl 1), R118-R120. <https://doi.org/10.1007/s004240000029>
- Roca, C., Requena, C., Sebastián-Pérez, V., Malhotra, S., Radoux, C., Pérez, C., Martínez, A., Antonio Páez, J., Blundell, T. L., & Campillo, N. E. (2018). Identification of new allosteric sites and modulators of AChE through computational and experimental tools. *J Enzyme Inhib Med Chem*, 33(1), 1034-1047. <https://doi.org/10.1080/14756366.2018.1476502>

Rotenberg, J. S., & Newmark, J. (2003). Nerve agent attacks on children: diagnosis and management. *Pediatrics*, 112(3 Pt 1), 648-658. <https://doi.org/10.1542/peds.112.3.648>

Russia responsible for Navalny poisoning, rights experts say.
(2021). <https://news.un.org/en/story/2021/03/1086012>

Sakayanathan, P., Loganathan, C., Kandasamy, S., Ramanna, R. V., Poomani, K., & Thayumanavan, P. (2019). In vitro and in silico analysis of novel astaxanthin-s-allyl cysteine as an inhibitor of butyrylcholinesterase and various globular forms of acetylcholinesterases. *Int J Biol Macromol*, 140, 1147-1157. <https://doi.org/10.1016/j.ijbiomac.2019.08.168>

Wani, T. A., Bakheit, A. H., Al-Majed, A. A., Altwaijry, N., Baquaysh, A., Aljuraissy, A., & Zargar, S. (2021). Binding and drug displacement study of colchicine and bovine serum albumin in presence of azithromycin using multispectroscopic techniques and molecular dynamic simulation. *J Mol Liq*, 333, 115934. <https://doi.org/10.1016/j.molliq.2021.115934>